IEEE Access
Multidisciplinary ⋮ Rapid Review ⋮ Open Access Journal

Received 29 November 2022, accepted 18 December 2022, date of publication 19 December 2022,
date of current version 27 December 2022.

Digital Object Identifier 10.1109/ACCESS.2022.3230915

RESEARCH ARTICLE

A Systematic and Comprehensive Geometric Framework for Multiphase Power Systems Analysis and Computing in Time Domain

AHMAD H. EID[1] AND FRANCISCO G. MONTOYA[2]
[1]Department of Electrical Engineering, Faculty of Engineering, Port-Said University, Port Fouad 42526, Egypt
[2]Department of Engineering, University of Almería, 04120 Almeria, Spain

Corresponding author: Francisco G. Montoya (pagilm@ual.es)

This work was supported in part by the Ministry of Science and Innovation under Grant PGC2018-098813-B-C33.

ABSTRACT This paper presents a new framework for a systematic and thorough generalization of the most well-known instantaneous transformations used in electrical engineering for power systems analysis and computing through geometric principles based on the language of Geometric Algebra. By introducing the concepts of Kirchhoff Vector and Kirchhoff Subspace, a new generalized transformation is presented. Thus, it is shown how the Clarke, Park or Hyper-Space vector transformations (widely used in electrical engineering) are particular cases of this unifying framework. Moreover, a generalization to an arbitrary number of phases is achieved. In order to be as close as possible to the geometrical intuition, all the underlying ideas are presented by means of spatial-like conceptualizations, substantiated by their corresponding algebraic formulation. This proposal has potential uses in a wide range of power system applications such as electrical machines, current compensation, power quality, electronic converters or transmission lines. Preliminary results show the superior efficiency of the method compared to matrix methods. Some real-world examples have been included to highlight the potential use of the method.

INDEX TERMS Geometric algebra, geometric electricity, sequence components, Clarke transformation, park transformation, hyper space vectors, Kirchhoff's laws.

I. INTRODUCTION

Tthe study of multiphase voltages or currents and their relationship is a topic of interest in several disciplines of electrical and power engineering such as active filtering [1], [2], electrical machines [3], transmission lines [4], control HVDC AC grids [5], frequency estimation and control [6], power converters [7] or microgrids [8]. In this context, matrix methods are used to solve the governing equations. The solution can be approached from an instantaneous (time-domain) or a complex-phasor (frequency-domain for sinusoidal supply) point of view. In general, existing methods aim at obtaining an orthogonal matrix-based transform under some custom predefined assumptions [9]. For example, matrix diagonalization and eigenvalue decomposition techniques are widely used as a starting point [10] to remove zero sequence component or to decouple variables. In this way, an algebraic and calculus derivation is obtained, but without a deeper understanding of the physical realm of the problem. For a complete understanding of the underlying principles, it is essential to adopt an approach that is much more closely linked to electrical practice and in clear connection with Kirchhoff's laws [11]. This paper attempts to provide a new vision based on these laws and founded on geometrically oriented principles strongly rooted in the engineering mindset [12]. The proposed methodology relies on a quite new framework based on Geometric Algebra (GA) to provide a clear spatial-like intuition, allowing a general understanding of the transformations for multiphase systems [13]. Recently, GA has been successfully applied by some authors to define a generalized concept of frequency [6], gaining new insights from a geometrical

The associate editor coordinating the review of this manuscript and approving it for publication was Zhouyang Ren.

perspective. Other applications to power systems [14], [15] or adaptive filtering [16] are also presented. A comprehensive list of application fields is detailed in [17] and [18]. The method presented here is named *Simple Kirchhoff Rotation* (SKR) framework. Founded on the roots of a previous work described in [13], a new general and efficient framework is presented. By general, it means that: 1) it applies to an unlimited number of phases without restriction (from two to n-phase systems) and 2) it unifies existing transformations like Clarke-Concordia [19], Park [20], Hyper-Space vectors [21] and others in purely time domain. By efficient, it means that it outperforms other existing matrix methods computationally.

The geometric operations presented in the proposed framework (simple rotations and projections) are universally sufficient to conceptualize all relevant geometry behind commonly used electrical transformations. The GA formulation of such geometric operations is much more natural compared to matrix formulations. This framework emphasises the geometry over the computation, as such, it is very important for younger engineers to intuitively understand the core concepts behind electrical transformations. Additionally, this unification of transformations in multiple dimensions has the potential to benefit the analysis of multi-phase systems of arbitrary complexity. Frequency approaches, like Fortescue's transformation, rely on complex phasors and will be analyzed in a separate paper.

A. CONTRIBUTIONS AND OUTLINE

This paper mainly contributes to the following topics:

- Definition of a new framework based on geometric principles rooted in the unified language of Geometric Algebra that applies to multiphase power systems dynamics and operations with an arbitrary number of phases.
- Generalization of time domain transformations like Clarke, Park, and Hyper-Space vector widely used in power systems through the proposed method known as *Simple Kirchhoff Rotation*. They are all particular cases of a superior and simple geometrical model obtained by rotations and projections in Euclidean space.
- Implementation of more efficient techniques for electrical transformations. For applications requiring only the basic geometric operation of rotating one vector to another, the use of rotation matrices or complex numbers is completely unnecessary, on both the levels of conceptual understanding and computational efficiency.
- Gradual Introduction of GA terminology as a comprehensive tool for solving general and multi-dimensional problems in power systems from a purely geometric point of view rather than an algebraic one.

The paper is organized as follows: Section II presents the minimum mathematical background necessary to understand the basics of Geometric Algebra. Section III defines the geometrical model used to describe a multiphase system.

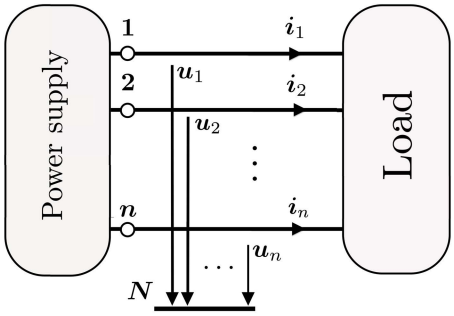

FIGURE 1. *n*-terminal electric circuit with *n* voltages u_i referenced to a virtual star point N and *n* currents i_i flowing through the terminals. Both currents and voltages fulfil Kirchhoff's laws.

Voltages and currents are transformed into vectors that can be manipulated in a Euclidean space through linear transformations. Traditional transformations are identified as geometric manipulations of vectors. Section IV presents the Simple Kirchhoff Rotation transformation and explains its structure and benefits as a generalization of rotations in a n-dimensional vector space. Section V presents some real-world cases where SKR is compared to other well-known methods in electrical engineering. Finally, section VI draws some conclusions about this work and proposes future ideas for ongoing papers.

II. MATHEMATICAL BACKGROUND

The ubiquitous use of matrices to represent linear transformations occasionally results in obscuring the geometric meaning behind them and consequently may lead to severing the deeper geometric connections between algebraic representations in engineering minds. This problem is amplified when combining matrices with complex numbers, as commonly applied in many engineering disciplines. Geometric algebra provides a powerful alternative to formulate geometric models in ways difficult to attain using matrices and complex numbers alone.

Many available references include sufficient explanations for the algebra and geometry behind GA, including [22], [23], and [24]. Introducing the full mathematical structure of GA in a limited space is extremely difficult. As such, the basic construction in the special case of 3 dimensions is included in Appendix A. The generalization to higher dimensions is provided in Appendix B along with well-known concepts like projections and rotations. Mathematics is also restricted to the minimum required for formulating our proposed geometric model later on.

III. THE BASIC GEOMETRIC MODEL

A. MODEL CONSTRUCTION FOR MULTIPHASE CIRCUITS

The basic geometric model constructed here assumes a n-terminal electric circuit (see Fig. 1) and that Kirchhoff's voltage and current laws apply to these terminals. A widely common and natural representation of the currents and voltages in such circuits involves the use of n coordinates or components for constructing the n-dimensional multiphase

voltage and current vector signal

$$\boldsymbol{x}(t) = [x_1(t), x_2(t), \ldots, x_n(t)] \tag{1}$$

Note that we use lower bold letters for representing vectors and upper bold letters for multivectors. Scalars are denoted by small non-bold letters. In GA language, the vector $\boldsymbol{x}(t)$ can be represented through a global frame using orthonormal basis vectors $\boldsymbol{\mu}_i$ (see Fig. 2)

$$\boldsymbol{x}\,(t) = \sum_{i=1}^{n} x_i\,(t)\,\boldsymbol{\mu}_i \tag{2}$$

For the sake of brevity, the time dependence will be omitted from now on. From Kirchhoff's current law, one can readily check that the sum of all terminal currents always satisfies $\sum_{m=1}^{n} i_m = 0$. For the voltage vector, a special node N (commonly known as virtual star point or virtual neutral) is introduced. Then, the voltage between each terminal m and the virtual star point N is defined. These new voltage quantities u_m have interesting properties [25] and also satisfy Kirchhoff's voltage law, $\sum_{m=1}^{n} u_m = 0$. The two Kirchhoff laws impose a geometric constraint on the voltage/current vector signal defined by (2) that can be expressed as an inner product:

$$\boldsymbol{x} \cdot \boldsymbol{k} = 0 \tag{3}$$

where

$$\boldsymbol{k} = \sum_{m=1}^{n} \boldsymbol{\mu}_m \tag{4}$$

We will call the special vector $\boldsymbol{k}$ the *Kirchhoff Vector* (KV), with the special property of having all components equal to one. The reader will probably identify that $\boldsymbol{k}$ resembles the more traditional vector form $\mathbf{1}_n = [1, 1, \ldots, 1]$. KV plays a significant geometric role in many multiphase sequence transformations as it geometrically captures the physical Kirchhoff constraints on multiphase signal vectors. Moreover, it represents the same 1D subspace that the traditional zero sequence component. The geometric meaning of identity (3) is that the multiphase signal vector $\boldsymbol{x}$ is always orthogonal to KV at any instant time. Another way to describe this property is by saying that $\boldsymbol{x}$ is always embedded in the $(n-1)$-dimensional subspace orthogonal to KV. In this work, the relation between a subspace $\mathcal{K}$ and a blade $\boldsymbol{K}$ (which algebraically represents it) is denoted by $\mathcal{K} \propto \boldsymbol{K}$. Accordingly, one can write $\mathcal{K} \propto \boldsymbol{k} \rfloor \boldsymbol{I}^{-1}$. As such, this subspace will be called the *Kirchhoff Subspace* (KS). We'll see in section IV, that it contains the typical α-β subspace along with other orthogonal 2D subspaces for dimensions greater than 3. Using GA, the KS can be represented algebraically by using the blade $\boldsymbol{K} = \boldsymbol{k} \rfloor \boldsymbol{I}^{-1}$ where $\boldsymbol{I} = \boldsymbol{\mu}_1 \boldsymbol{\mu}_2 \cdots \boldsymbol{\mu}_n = \boldsymbol{\mu}_{1,2,\ldots,n}$ is the so-called *phase space* pseudo-scalar. In the language of GA, the KV and KS blade are dual (or orthogonal complements) of each other. For a better comprehension of each of these components, the KS and KV are represented in Fig. 3 for a 3-dimensional space.

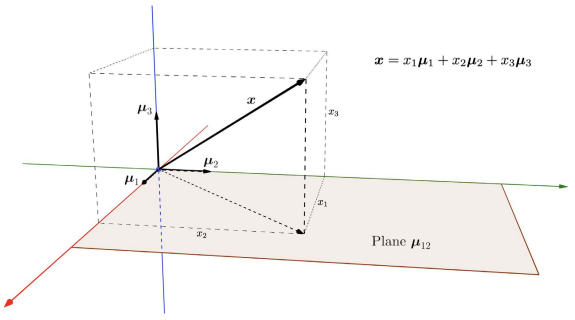

FIGURE 2. Vector representation of a multiphase signal x in an orthonormal basis frame μ_i. Each phase quantity x_i is a coordinate of the vector x.

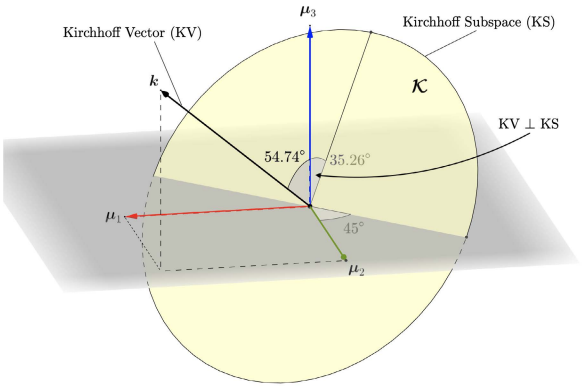

FIGURE 3. Geometric representation of the Kirchhoff Vector (KV) and Kirchhoff Subspace (KS). Both objects are dual to each other (orthogonal complement).

One of the basic goals of many sequence transformations is to express the n-dimensional signal vector $\boldsymbol{x}$ using a simpler $(n-1)$-dimensional coordinates frame that spans the KS. In this work, a class of transformations capable of attaining this goal is defined and it is known as *Kirchhoff Transformation* (KT). A KT is a linear operator T that performs two basic operations: 1) it maps the KV into a scaled version of an arbitrarily selected base vector $\boldsymbol{\mu}_i$, and 2) it maps the KS into the axis-aligned $(n-1)$-dimensional subspace $\mathcal{U}$ spanned by the remaining basis vectors $\boldsymbol{\mu}_j$ with $j \neq i$. Without loss of generality, we will assume $i = n$ for the remaining of this work, and consequently, $\mathcal{U}$ will be spanned by $\{\boldsymbol{\mu}_1, \boldsymbol{\mu}_2, \ldots, \boldsymbol{\mu}_{n-1}\}$. The above can be expressed as

$$\mathrm{T} : \boldsymbol{k} \mapsto \lambda \boldsymbol{\mu}_n \quad \text{or} \quad \mathrm{T} : \mathcal{K} \mapsto \mathcal{U}$$

where $\lambda \in \mathbb{R}$ is a scalar number. Applying the KT to the instantaneous multiphase signal vector $\boldsymbol{x}$, the transformed vector $\boldsymbol{y} = \mathrm{T}[\boldsymbol{x}] = \sum_{i=1}^{n} y_i \boldsymbol{\mu}_i$ is obtained. Because $\boldsymbol{x}$ always lies in the KS, the corresponding transformed vector $\boldsymbol{y}$ will be explicitly included in the subspace $\mathcal{U}$, with a zero-valued component y_n in the direction of $\boldsymbol{\mu}_n$.

B. THE UNIFORMLY-SPACED KIRCHHOFF FRAME

The representation of the geometric construction presented in the above section requires defining a suitable coordinate

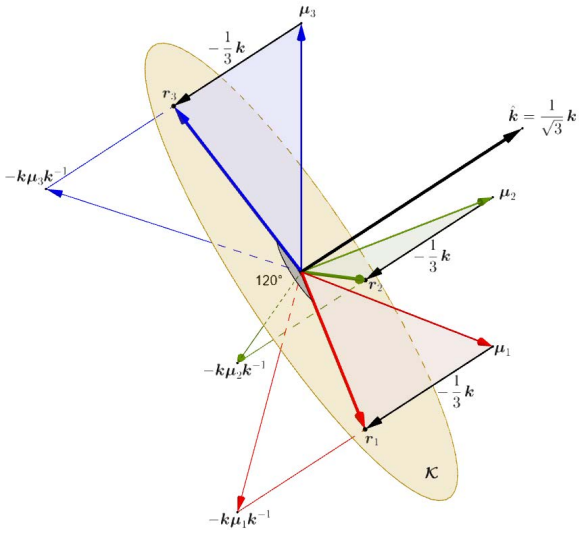

FIGURE 4. Construction of the uniformly-spaced Kirchhoff frame $\{r_1, r_2, r_3\}$ in 3-dimensions.

frame for the KS. Traditionally, power engineers have made use of a linearly dependent oblique frame $\{\boldsymbol{r}_i\}$ that spans KS. This frame is simply the projection of $\{\boldsymbol{\mu}_i\}$ into KS. In GA, the above can be accomplished through the linear projection operator [26]:

$$\boldsymbol{r}_i = \frac{1}{2}\left(\boldsymbol{\mu}_i - \boldsymbol{k}\boldsymbol{\mu}_i\boldsymbol{k}^{-1}\right) = \boldsymbol{\mu}_i - \frac{1}{n}\boldsymbol{k} = \boldsymbol{\mu}_i - \frac{1}{\sqrt{n}}\hat{\boldsymbol{k}} \tag{5}$$

where $\hat{\boldsymbol{k}} = \frac{1}{\|\boldsymbol{k}\|}\boldsymbol{k} = \frac{1}{\sqrt{n}}\boldsymbol{k}$ is the unit Kirchhoff vector. Deduction of relation (5) is also possible using the traditional vector rejection of $\boldsymbol{\mu}_i$ on $\boldsymbol{k}$:

$$\boldsymbol{r}_i = \boldsymbol{\mu}_i - \frac{\boldsymbol{\mu}_i \cdot \boldsymbol{k}}{\boldsymbol{k} \cdot \boldsymbol{k}}\boldsymbol{k} = \boldsymbol{\mu}_i - \frac{1}{n}\boldsymbol{k} \tag{6}$$

Fig. 4 shows a geometric representation for the 3D case. In addition to being simple to compute using GA, the frame $\{\boldsymbol{r}_i\}$ has several interesting properties. First, all vectors $\boldsymbol{r}_i$ have equal length $\|\boldsymbol{r}_i\| = \sqrt{\frac{n-1}{n}}$ and are orthogonal to the KV:

$$\boldsymbol{r}_i \cdot \boldsymbol{k} = \left(\boldsymbol{\mu}_i - \frac{1}{n}\boldsymbol{k}\right) \cdot \boldsymbol{k}\boldsymbol{\mu}_i \cdot \boldsymbol{k} - \frac{1}{n}\boldsymbol{k} \cdot \boldsymbol{k} = 1 - \frac{1}{n}n = 0 \tag{7}$$

Accordingly, applying the KT to vectors $\boldsymbol{r}_i$ results in a set of vectors $\boldsymbol{s}_i = \mathrm{T}[\boldsymbol{r}_i]$ in the subspace $\mathcal{U}$. Second, the angle between any pair of vectors $\boldsymbol{r}_i, \boldsymbol{r}_j$ is constant $\varphi = \cos^{-1}\frac{\boldsymbol{r}_i \cdot \boldsymbol{r}_j}{\|\boldsymbol{r}_i\|\|\boldsymbol{r}_j\|} = \cos^{-1}\frac{1}{1-n}$, which implies that vectors $\boldsymbol{r}_i$ are uniformly distributed in KS. For example, in a three-wire system, $n = 3$ and $\varphi = 120°$. Third, we can discard one arbitrary vector, say $\boldsymbol{r}_n$, to obtain a linearly independent basis $\{\boldsymbol{r}_1, \boldsymbol{r}_2, \ldots, \boldsymbol{r}_{n-1}\}$ spanning KS. This basis can be orthonormalized, using Gram-Schmidt or any other similar procedure, and complemented with the unit KV, i.e., $\hat{\boldsymbol{k}} = \frac{1}{\sqrt{n}}\boldsymbol{k}$ to obtain a full orthonormal basis $\{\boldsymbol{c}_1, \boldsymbol{c}_2, \ldots, \boldsymbol{c}_{n-1}, \boldsymbol{c}_n\}$ for the n-dimensional phase signal space, also spanned by $\{\boldsymbol{\mu}_i\}$. Note that $\boldsymbol{c}_n = \hat{\boldsymbol{k}}$. Due to these properties, $\{\boldsymbol{r}_i\}$ will be called the Uniformly-spaced Kirchhoff Frame (UKF). The use of the KV and UKF makes it simple to test if a given transformation, expressed as a square matrix, is a KT. The $n \times n$ square matrix $M = \begin{pmatrix}\boldsymbol{m}_1 & \boldsymbol{m}_2 & \cdots & \boldsymbol{m}_n\end{pmatrix}$ having column vectors $\boldsymbol{m}_i$ represents a KT if and only if the following two conditions hold for some fixed j and all i:

$$\sum_{q=1}^{n}\boldsymbol{m}_q = \lambda\boldsymbol{\mu}_j \qquad \boldsymbol{m}_i \cdot \boldsymbol{\mu}_j = \frac{\lambda}{n} \tag{8}$$

The first condition (8) results from the KT property $\mathrm{T} : \boldsymbol{k} \mapsto \lambda\boldsymbol{\mu}_j$ for some j. In the case of M representing T, then:

$$\begin{aligned}\mathrm{T}[\boldsymbol{k}] = M\boldsymbol{k} &= \begin{pmatrix}\boldsymbol{m}_1 & \boldsymbol{m}_2 & \cdots & \boldsymbol{m}_n\end{pmatrix}\begin{pmatrix}1 & 1 & \cdots\end{pmatrix}^T \\ &= \sum_{q=1}^{n}\boldsymbol{m}_q = \lambda\boldsymbol{\mu}_j\end{aligned} \tag{9}$$

The second condition (8) results from the KT property $\mathrm{T} : \mathcal{K} \mapsto \mathcal{U}$. This property implies that a UKF vector $\boldsymbol{r}_i$ in $\mathcal{K}$ is transformed into a vector $\boldsymbol{s}_i = \mathrm{T}[\boldsymbol{r}_i]$ in $\mathcal{U}$, which is by definition orthogonal to $\boldsymbol{\mu}_j$. Accordingly, this property can be expressed as $\mathrm{T}[\boldsymbol{r}_i] \cdot \boldsymbol{\mu}_j = 0$ for all $i = 1, 2, \ldots, n$. Expressing $\mathrm{T}[\boldsymbol{r}_i]$ using matrix M gives:

$$\begin{aligned}\mathrm{T}[\boldsymbol{r}_i] = M\boldsymbol{r}_i &= M\left(\boldsymbol{\mu}_i - \frac{1}{n}\boldsymbol{k}\right) \\ &= M\boldsymbol{\mu}_i - \frac{1}{n}M\boldsymbol{k} = \boldsymbol{m}_i - \frac{\lambda}{n}\boldsymbol{\mu}_j\end{aligned} \tag{10}$$

which leads to:

$$\mathrm{T}[\boldsymbol{r}_i] \cdot \boldsymbol{\mu}_j = \left(\boldsymbol{m}_i - \frac{\lambda}{n}\boldsymbol{\mu}_j\right) \cdot \boldsymbol{\mu}_j = \boldsymbol{m}_i \cdot \boldsymbol{\mu}_j - \frac{\lambda}{n} = 0 \tag{11}$$

Note that the second condition in (8) is equivalent to the j-th row vector of M being equal to $\frac{\lambda}{n}\boldsymbol{k}$; yet another relation depending on the KV.

C. CLARKE AND PARK MATRICES AS KIRCHHOFF TRANSFORMATIONS

In the case of a three-phase system, the power-invariant form of the Clarke transformation matrix is:

$$C = \sqrt{\frac{2}{3}}\begin{pmatrix}1 & -\frac{1}{2} & -\frac{1}{2} \\ 0 & \frac{\sqrt{3}}{2} & -\frac{\sqrt{3}}{2} \\ \frac{1}{\sqrt{2}} & \frac{1}{\sqrt{2}} & \frac{1}{\sqrt{2}}\end{pmatrix} \tag{12}$$

Summing its column vectors one gets $\boldsymbol{m}_1 + \boldsymbol{m}_2 + \boldsymbol{m}_3 = \sqrt{3}\boldsymbol{\mu}_3$, meaning that in this case $j = 3$ and $\lambda = \sqrt{3}$. Additionally, the third row of C contains the quantities $\boldsymbol{m}_i \cdot \boldsymbol{\mu}_3 = \frac{\lambda}{n} = \frac{\sqrt{3}}{3} = \frac{1}{\sqrt{3}}$ as expected. The Park transformation defines a continuous rotation at an arbitrary frequency ω. It is composed of the $dq0$ matrix D

$$D = \begin{pmatrix}\cos\omega t & \sin\omega t & 0 \\ -\sin\omega t & \cos\omega t & 0 \\ 0 & 0 & 1\end{pmatrix} \tag{13}$$

and the Clarke matrix C, yielding the single matrix:

$$P = DC$$

$$= \sqrt{\frac{2}{3}} \begin{pmatrix} \cos\theta & \cos(\theta-\varphi) & \cos(\theta+\varphi) \\ -\sin\theta & -\sin(\theta-\varphi) & -\sin(\theta+\varphi) \\ \frac{1}{\sqrt{2}} & \frac{1}{\sqrt{2}} & \frac{1}{\sqrt{2}} \end{pmatrix} \quad (14)$$

with $\theta = \omega t$ and $\varphi = \frac{2}{3}\pi$. Again, summing its column vectors one gets $\boldsymbol{m}_1 + \boldsymbol{m}_2 + \boldsymbol{m}_3 = \sqrt{3}\boldsymbol{\mu}_3$, Additionally, the third row of P contains the quantities $\boldsymbol{m}_i \cdot \boldsymbol{\mu}_3 = \frac{\lambda}{n} = \frac{\sqrt{3}}{3} = \frac{1}{\sqrt{3}}$ as expected from the Kirchhoff transformation.

D. HYPER-SPACE VECTORS MATRIX AS KIRCHHOFF TRANSFORMATION

In [27] a general formulation of the Fryze-Buchholz-Depenbrock (FBD) transformation is developed based on linear algebra. A matrix H with a predefined structure is constructed to represent the required transformation. The Kirchhoff constraint is imposed as the identity $H\boldsymbol{k} = \boldsymbol{0}$. The H matrix is $(n-1) \times n$ where row number r starts with $r-1$ leading zeros, then element (r, r) contains the value $\frac{\sqrt{n-r}}{\sqrt{n-r+1}}$, followed by the repeated value $\frac{-1}{\sqrt{(n-r)(n-r+1)}}$ for the remaining columns in the same row r. In this work, we will augment the matrix H with a final row of zeros to make it a square matrix. The following is an example for $n = 4$:

$$H = \begin{pmatrix} \sqrt{\frac{3}{4}} & \frac{-1}{\sqrt{12}} & \frac{-1}{\sqrt{12}} & \frac{-1}{\sqrt{12}} \\ 0 & \sqrt{\frac{2}{3}} & \frac{-1}{\sqrt{6}} & \frac{-1}{\sqrt{6}} \\ 0 & 0 & \sqrt{\frac{1}{2}} & \frac{-1}{\sqrt{2}} \\ 0 & 0 & 0 & 0 \end{pmatrix} \quad (15)$$

By investigating the column vectors $\boldsymbol{h}_i$ of H, we find they are all of the same length $\|\boldsymbol{h}_i\| = \sqrt{\frac{n-1}{n}}$, and orthogonal to the basis vector $\boldsymbol{\mu}_n$ as evident by the final zero in each $\boldsymbol{h}_i$. In addition, the angle between any pair of column vectors $\boldsymbol{h}_i, \boldsymbol{h}_j$ is constant $\varphi = \cos^{-1}\frac{1}{1-n}$, meaning that vectors $\boldsymbol{h}_i$ are uniformly distributed in the subspace $\mathcal{U}$ spanned by $\{\boldsymbol{\mu}_1, \boldsymbol{\mu}_2, \ldots, \boldsymbol{\mu}_{n-1}\}$. These are very similar properties to the UKF vectors $\boldsymbol{r}_i$ which span the KS. The geometric meaning of the transformation H represents is clear: it projects the frame $\{\boldsymbol{\mu}_i\}$ onto the KS to obtain the UKF $\{\boldsymbol{r}_i\}$, then applies a rotation transformation T_{rh} to rotate the UKF $\{\boldsymbol{r}_i\}$ into the hyper-space vectors frame $\{\boldsymbol{h}_i\}$. Since $\{\boldsymbol{r}_i\}$ spans the KS, while $\{\boldsymbol{h}_i\}$ spans $\mathcal{U}$, we can conclude that the rotation T_{rh} is itself a Kirchhoff transformation.

IV. SIMPLE KIRCHHOFF ROTATION TRANSFORMATION

Rotations in 2 and 3 dimensions are simple and easy to visualize. However, this is not the case for 4 and higher dimensions, which are generally non-simple [28]. A general rotation in n dimensions is a composite of $\frac{n}{2}$ (for even n) or $\frac{n-1}{2}$ (for odd n) simple rotations; a direct result of the Cartan-Dieudonné theorem [29]. Each simple rotation is completely defined by an angle and a plane of rotation. For a general rotation, the corresponding planes of simple rotations are orthogonal. In matrix algebra, the eigendecomposition of a rotation matrix can be used to compute the angle-plane elements of its simple rotations. Generalizations of Clarke

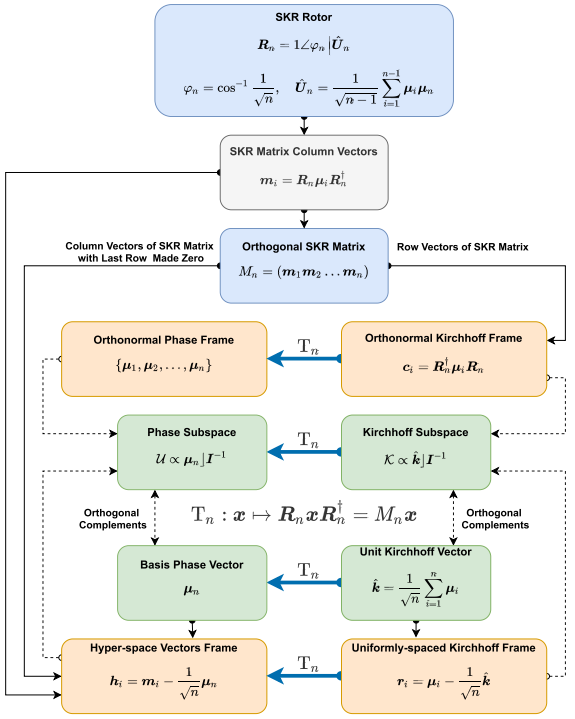

FIGURE 5. Summary of the proposed Simple Kirchhoff Rotation (SKR) framework.

matrices [9] to higher dimensions are typically general non-simple rotations. Interestingly enough, the use of GA enables the formulation of a new kind of Kirchhoff transformation, while completely avoiding the use of intermediate frames of any sort. The new transformation we propose performs a rotation in n-dimensional phase space formulated using the so-called *simple geometric rotors* in GA (from now on, we use the word *geometric rotor* for simplicity). Note that *geometric rotors* are even multivectors that perform rotations to vectors and multivectors in any dimension. It satisfies the two properties of KT.

A. PROPOSED METHOD

In this work, a new general method is proposed to unify electrical transformations based on geometrical principles. It will be referred to as Simple Kirchhoff Rotation (SKR). Fig. 5 is a summary of the proposed SKR framework. The SKR transformation $\mathbf{T}_n : \mathcal{K} \to \mathcal{U}$ can be represented either using a GA rotor $\boldsymbol{R}_n$, where $\mathbf{T}_n[\boldsymbol{x}] = \boldsymbol{R}_n\boldsymbol{x}\tilde{\boldsymbol{R}}_n^{\dagger}$, or using an orthogonal matrix $M_n = (\boldsymbol{m}_1\boldsymbol{m}_2\cdots\boldsymbol{m}_n)$, where $\mathbf{T}_n[\boldsymbol{x}] = M_n\boldsymbol{x}$. The row vectors $\boldsymbol{c}_i$ of M_n constitute the orthonormal Kirchhoff frame satisfying $\mathbf{T}_n[\boldsymbol{c}_i] = \boldsymbol{\mu}_i$. The $n-1$ dimensional phase subspace $\mathcal{U}$ can be represented using the orthogonal complement $\boldsymbol{\mu}_n \rfloor \boldsymbol{I}^{-1}$ of the basis vector $\boldsymbol{\mu}_n$. The $n-1$ dimensional Kirchhoff subspace $\mathcal{K}$ can be represented using the orthogonal complement $\hat{\boldsymbol{k}} \rfloor \boldsymbol{I}^{-1}$ of the unit vector $\hat{\boldsymbol{k}} = \frac{1}{\sqrt{n}}\sum_{i=1}^{n}\boldsymbol{\mu}_i$. The two subspaces are also related through the SKR using $\mathbf{T}_n[\boldsymbol{x}] = \boldsymbol{y} \in \mathcal{U}$ for all $\boldsymbol{x} \in \mathcal{K}$. Finally, the SKR relates the uniformly-spaced Kirchhoff frame vectors $\boldsymbol{r}_i = \boldsymbol{\mu}_i - \frac{1}{\sqrt{n}}\hat{\boldsymbol{k}}$, which span $\mathcal{K}$, with the

hyper-space frame vectors $\boldsymbol{h}_i = \boldsymbol{m}_i - \frac{1}{\sqrt{n}}\hat{\boldsymbol{\mu}}_i$, which span $\mathcal{U}$, through $\mathbf{T}_n[\boldsymbol{r}_i] = \boldsymbol{h}_i$. The hyperspace frame vectors $\boldsymbol{h}_i$ can also be read directly as the column vectors of M_n with the last row replaced by zeros.

In GA, simple rotations are represented by *geometric rotors*, constructed from two conveniently chosen vectors. Following the first Kirchhoff transformation property $\boldsymbol{k} \mapsto \lambda\boldsymbol{\mu}_n$, we take the two vectors to be the unit KV, i.e., $\hat{\boldsymbol{k}} = \frac{1}{\sqrt{n}}\boldsymbol{k}$ and the basis vector $\boldsymbol{\mu}_n$. Because rotations preserve orthogonality, the simple *geometric rotor* also satisfies the second Kirchhoff transformation property $\mathcal{K} \mapsto \mathcal{U}$. The SKR *geometric rotor* $\boldsymbol{R}_n$ can be defined as:

$$\begin{aligned}\boldsymbol{R}_n &= \sqrt{\frac{1}{2}+\frac{1}{2}\hat{\boldsymbol{k}}\cdot\boldsymbol{\mu}_n}+\sqrt{\frac{1}{2}-\frac{1}{2}\hat{\boldsymbol{k}}\cdot\boldsymbol{\mu}_n}\frac{\hat{\boldsymbol{k}}\wedge\boldsymbol{\mu}_n}{\left\|\hat{\boldsymbol{k}}\wedge\boldsymbol{\mu}_n\right\|}\\ &= \sqrt{\frac{1}{2}+\frac{1}{2\sqrt{n}}}-\frac{1}{\sqrt{n-1}}\sqrt{\frac{1}{2}-\frac{1}{2\sqrt{n}}}\sum_{i=1}^{n-1}\boldsymbol{\mu}_i\boldsymbol{\mu}_n\\ &= e^{\left(-\frac{1}{2}\cos^{-1}\frac{1}{\sqrt{n}}\right)\left(\frac{1}{\sqrt{n-1}}\sum_{i=1}^{n-1}\boldsymbol{\mu}_i\boldsymbol{\mu}_n\right)}\\ &= 1\angle-\cos^{-1}\frac{1}{\sqrt{n}}\left|\sum_{i=1}^{n-1}\left(\frac{1}{\sqrt{n-1}}\right)_{i,n}\right.\end{aligned} \tag{16}$$

The SKR *geometric rotor* $\boldsymbol{R}_n$ has a rotation angle of

$$\varphi_n = -\cos^{-1}\frac{1}{\sqrt{n}} \tag{17}$$

and a rotation plane represented by the bivector

$$\boldsymbol{B}_n = \frac{1}{\sqrt{n-1}}\sum_{i=1}^{n-1}\boldsymbol{\mu}_i\boldsymbol{\mu}_n \tag{18}$$

generated by the two unit vectors $\frac{1}{\sqrt{n-1}}\sum_{i=1}^{n-1}\boldsymbol{\mu}_i$ and $\boldsymbol{\mu}_n$. A multiphase signal vector $\boldsymbol{x}$ can be transformed by the SKR *geometric rotor* using the sandwich geometric product:

$$\mathrm{T}:\boldsymbol{x}\mapsto\boldsymbol{R}_n\boldsymbol{x}\boldsymbol{R}_n^{\dagger} \tag{19}$$

Additionally, one can easily construct the orthogonal rotation matrix M_n where $M_n^{-1} = M_n^T$ for this SKR having column vectors $\boldsymbol{m}_i$ defined from the SKR *geometric rotor* using:

$$M_n = \left(\boldsymbol{m}_1\ \boldsymbol{m}_2\ \cdots\ \boldsymbol{m}_n\right) \tag{20}$$

$$\boldsymbol{m}_i = \boldsymbol{R}_n\boldsymbol{\mu}_i\boldsymbol{R}_n^{\dagger} \tag{21}$$

The structure of matrix M_n is the following:

$$M_n = \begin{pmatrix} a_n & b_n & \dots & \dots & b_n & -c_n\\ b_n & a_n & b_n & \dots & b_n & -c_n\\ \vdots & & & & & \\ b_n & b_n & \dots & \dots & a_n & -c_n\\ c_n & c_n & \dots & \dots & c_n & c_n \end{pmatrix} \tag{22}$$

with

$$a_n = 1-\frac{1}{n+\sqrt{n}}$$

$$b_n = -\frac{1}{n+\sqrt{n}}$$

$$c_n = \frac{1}{\sqrt{n}}$$

The SKR structure can be analysed in terms of eigenvalues and eigenvectors. It can be proved that there are $n-2$ real eigenvalues with value $\lambda_i = a_i - b_i = 1$ with $i = 1\dots n-2$. Only λ_{n-1} and λ_n are complex conjugate eigenvalues.

1) THREE-DIMENSIONAL CASE

Three-phase power systems can be considered from a 3- or 4-dimensional standpoint depending on the specific application [30]. For the case of 3 dimensions, 3×3 matrices are typically used as in Clarke or Park transformations. Based on eq. (16), SKR *geometric rotor* $\boldsymbol{R}_n$ for $n = 3$ can be obtained as

$$\begin{aligned}\boldsymbol{R}_3 &= 1\angle-54.74^\circ\left|\begin{matrix}\left(\frac{1}{\sqrt{2}}\right)_{1,3}\\ \left(\frac{1}{\sqrt{2}}\right)_{2,3}\end{matrix}\right.\\ &= \cos(-\frac{54.74}{2})+\frac{\sin(-\frac{54.54}{2})}{\sqrt{2}}\left(\boldsymbol{\mu}_1\boldsymbol{\mu}_3+\boldsymbol{\mu}_2\boldsymbol{\mu}_3\right)\\ &= 0.888-0.325\boldsymbol{\mu}_{1,3}-0.325\boldsymbol{\mu}_{2,3}\end{aligned} \tag{23}$$

and by considering (22), the matrix M_3 can be obtained as:

$$M_3 = \begin{pmatrix} a_3 & b_3 & -c_3\\ b_3 & a_3 & -c_3\\ c_3 & c_3 & c_3\end{pmatrix}$$

$$a_3 = 1-\frac{1}{3+\sqrt{3}},\ b_3 = -\frac{1}{3+\sqrt{3}},\ c_3 = \frac{1}{\sqrt{3}}$$

We can construct an orthonormal frame $\{\boldsymbol{c}_i\}$ for the KS by rotating the $\{\boldsymbol{\mu}_i\}$ frame using the inverse of the SKR and $\boldsymbol{c}_i = \boldsymbol{R}_n^{\dagger}\boldsymbol{\mu}_i\boldsymbol{R}_n$. By simple inspection, one can observe that vectors $\boldsymbol{c}_i$ are exactly the row vectors of the SKR matrix M_n, as it's a rotation matrix satisfying $M_n^{-1} = M_n^T$. Fig. 6 illustrates the orthonormal frame $\{\boldsymbol{c}_1, \boldsymbol{c}_2, \boldsymbol{c}_3\}$ in 3 dimensions.

It is interesting to note that the SKR rotor/matrix is different from that of Clarke as shown in [30]

$$\begin{aligned}\boldsymbol{R}_C &= 0.8805+0.1159\boldsymbol{\mu}_{1,2}-0.3647\boldsymbol{\mu}_{1,3}-0.2798\boldsymbol{\mu}_{2,3}\\ &= 0.8805+0.474\left(0.24\boldsymbol{\mu}_{1,2}-0.59\boldsymbol{\mu}_{2,3}-0.77\boldsymbol{\mu}_{1,3}\right)\\ &= e^{28.3\left(0.24\boldsymbol{\mu}_{1,2}-0.77\boldsymbol{\mu}_{1,3}-0.59\boldsymbol{\mu}_{2,3}\right)}\\ &= 1\angle-56.6^\circ\left|\begin{matrix}\frac{\sqrt{2}+2}{\sqrt{8\sqrt{3}+2+18}}\boldsymbol{\mu}_{1,3}\\ \frac{1}{\sqrt{4\sqrt{3}+2+9}}\boldsymbol{\mu}_{1,3}\\ \frac{\sqrt{2}+\sqrt{3}}{\sqrt{4\sqrt{3}+2+9}}\boldsymbol{\mu}_{2,3}\end{matrix}\right.\end{aligned} \tag{24}$$

Note that, in three dimensions, both Clarke and SKR method lead to the full diagonalization of the typical matrices that appears in electrical machines or transmission line

problems. For example, for an inductance matrix

$$L = \begin{pmatrix} L_p & L_m & L_m \\ L_m & L_p & L_m \\ L_m & L_m & L_p \end{pmatrix}$$

we get the following result

$$L_T = CLC^{-1} = M_3 L M_3^{-1} = \begin{bmatrix} L_\alpha & 0 & 0 \\ 0 & L_\beta & 0 \\ 0 & 0 & L_0 \end{bmatrix} \tag{25}$$

where $L_\alpha = L_\beta = L_p - L_m$ and $L_0 = L_p + 2L_m$. We prove in Appendix D that there is a whole family of rotations that map the basis vector $\boldsymbol{\mu}_3$ to the Kirchhoff vector $\hat{\boldsymbol{k}}$. The simplest of them is the one provided by the SKR method. Moreover, by inspecting EQs. (23) and (12), it is noted that the SKR method uses fewer parameters than Clarke/Park method. Therefore, potential advantages from a computational point of view are foreseen. Section IV-B presents evidence to support this claim.

2) FOUR-DIMENSIONAL CASE

For three-phase systems with four wires or four-phase systems without neutral wire, the SKR geometric rotor is:

$$\boldsymbol{R}_4 = 1\angle -60° \left| \begin{matrix} \left(\frac{1}{\sqrt{3}}\right)_{1,4} \\ \left(\frac{1}{\sqrt{3}}\right)_{2,4} \\ \left(\frac{1}{\sqrt{3}}\right)_{3,4} \end{matrix} \right.$$

$$M_4 = \begin{pmatrix} a_4 & b_4 & b_4 & -c_4 \\ b_4 & a_4 & b_4 & -c_4 \\ b_4 & b_4 & a_4 & -c_4 \\ c_4 & c_4 & c_4 & c_4 \end{pmatrix}$$

$$a_4 = \frac{5}{6}, \quad b_4 = -\frac{1}{6}, \quad c_4 = \frac{1}{2}$$

Additionally, the column vectors $\boldsymbol{h}_i$ of a related hyper-space matrix $H_n = \begin{pmatrix} \boldsymbol{h}_1 & \boldsymbol{h}_2 & \cdots & \boldsymbol{h}_n \end{pmatrix}$ can be constructed by rotating the UKF vectors $\boldsymbol{r}_i = \boldsymbol{\mu}_i - \frac{1}{n}\boldsymbol{k}$ using the SKR. This is because the SKR, being a rotation, rotates vectors in the KS into vectors in the phase subspace $\mathcal{U}$ while preserving their angles and lengths. Fig. 7 illustrates the UKF $\{\boldsymbol{r}_1, \boldsymbol{r}_2, \boldsymbol{r}_3\}$ and hyper-space vectors frame $\{\boldsymbol{h}_1, \boldsymbol{h}_2, \boldsymbol{h}_3\}$ in 3 dimensions. The final expression for computing the corresponding hyper-space vectors matrix is simple: H_n is exactly M_n with the final row made zero. This is evident from the following:

$$\boldsymbol{h}_i = \boldsymbol{R}_n \boldsymbol{r}_i \boldsymbol{R}_n^\dagger = \boldsymbol{R}_n \left(\boldsymbol{\mu}_i - \frac{1}{n}\boldsymbol{k}\right) \boldsymbol{R}_n^\dagger = \boldsymbol{R}_n \boldsymbol{\mu}_i \boldsymbol{R}_n^\dagger - \frac{1}{n}\boldsymbol{R}_n \boldsymbol{k} \boldsymbol{R}_n^\dagger$$
$$= \boldsymbol{m}_i - \frac{\sqrt{n}}{n}\boldsymbol{R}_n \hat{\boldsymbol{k}} \boldsymbol{R}_n^\dagger = \boldsymbol{m}_i - \frac{1}{\sqrt{n}}\boldsymbol{\mu}_n$$

B. COMPUTATIONAL COMPLEXITY OF SKR METHOD

One of the main advantages of the SKR method over traditional methods is that it provides a unifying framework

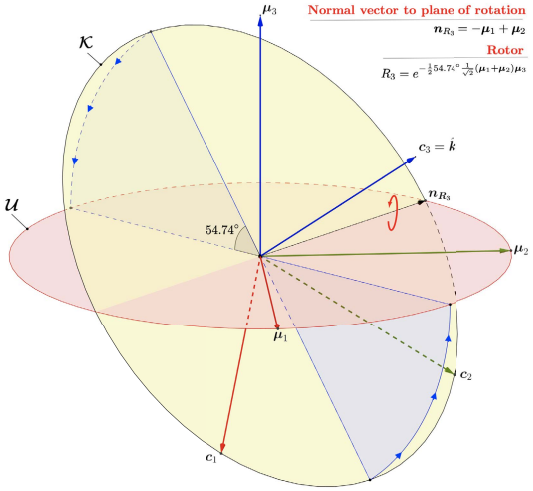

FIGURE 6. The simple Kirchhoff *geometric rotor* R_3 and corresponding orthonormal Kirchhoff frame $\{c_1, c_2, c_3\}$ in 3-dimensions.

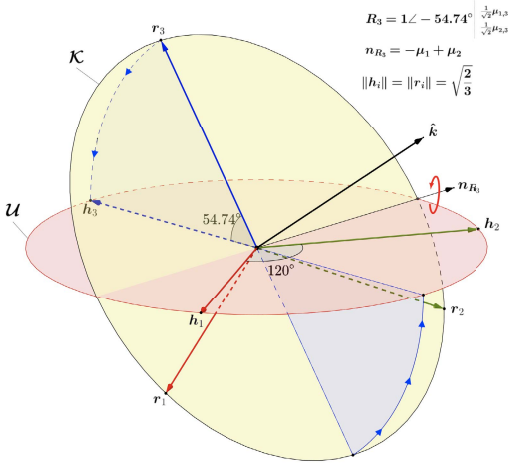

FIGURE 7. The simple *geometric rotor* R_3 and corresponding uniformly-spaced Kirchhoff frame $\{r_1, r_2, r_3\}$ and hyper-space vectors frame $\{h_1, h_2, h_3\}$ in 3D.

to think intuitively, formally and generally about transformations in power systems. Its simplicity is revealed by equation (16), irrespective of the number of dimensions to be considered. However, the above does not guarantee that SKR is computationally efficient and, therefore, useful to the engineer for its application in realistic systems. Therefore, a series of tests have been carried out to verify the superiority of the method over Clarke's method, as one the most widely used by the community.

The setup consisted of applying both methods to a set of 1000 random voltage vectors, transforming the phase values to modal components. For this purpose, an Intel i7 workstation processor with 32 GBytes RAM has been used and the implementation has been carried out using C# language. The results obtained are shown in table 1. Notice how the SKR method has higher computational performance

TABLE 1. Processing time to transform 1000 random vectors by the clarke and SKR method.

	Time (μs)			Time (μs)	
Dimension	Clarke	SKR	Dimension	Clarke	SKR
3	27.86	12.20	26	807.01	47.32
4	36.71	13.28	27	866.16	49.82
5	48.36	13.62	28	927.97	51.64
6	61.47	14.39	29	993.14	54.84
7	77.13	15.22	30	1,057.39	56.34
8	94.84	16.14	31	1,126.57	57.90
9	115.63	17.08	32	1,198.33	60.47
10	143.92	17.78	33	1,246.67	62.13
11	168.43	19.47	34	1,492.63	61.23
12	194.32	19.77	35	1,399.00	63.22
13	222.83	21.21	36	1,476.99	63.90
14	254.37	22.43	37	1,556.56	65.98
15	294.58	23.88	38	1,637.59	67.20
16	329.18	25.07	39	1,953.26	69.39
17	367.77	27.56	40	1,812.72	71.17
18	408.30	30.61	41	2,112.17	72.29
19	448.45	30.91	42	2,208.85	74.03
20	490.91	33.10	43	2,313.42	75.88
21	534.98	34.85	44	2,174.11	76.77
22	583.19	38.36	45	2,281.55	79.43
23	633.23	39.05	46	2,374.46	80.74
24	687.15	41.26	47	2,464.54	81.08
25	740.86	43.89	48	2,570.13	82.74

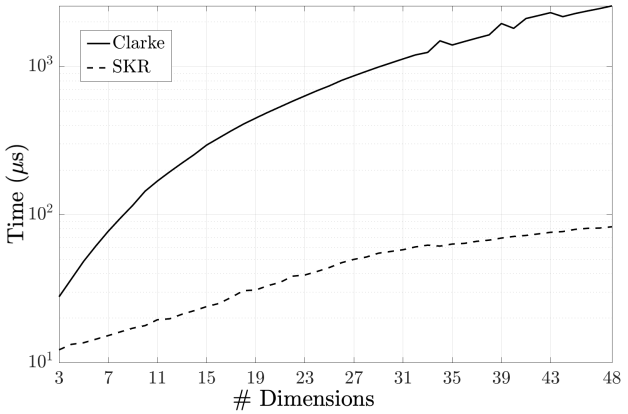

FIGURE 8. Performance comparison among Clarke and SKR method for data in table 1.

than Clarke. For reduced dimensions, i.e. 3 dimensions, Clarke is 128.36% worse than SKR. As the number of dimensions increases, the computational complexity of Clarke's method increases exponentially, while the SKR method increases linearly (see figure 8). For example, for a 15-phase system, Clarke is 1133.6% slower than SKR. Note that Clarke's implementation has been realised using standard matrix-vector multiplication methods which require two nested loops. In contrast, a simple vector relation has been used for the SKR implementation, which only uses a single loop and is much more efficient. Assume a vector $\boldsymbol{x}$ in n-dimensional space. Assume $\boldsymbol{R}$ is the SKR rotor for this space which rotates basis vector $\boldsymbol{\mu}_n$ to the unit Kirchhoff vector $\hat{\boldsymbol{k}}$, then the rotated vector $\boldsymbol{x}_R$ can be expressed compactly using simple vector operations as follows:

$$\boldsymbol{x}_R = \boldsymbol{R}\boldsymbol{x}\boldsymbol{R}^{\dagger} = \boldsymbol{x} + \left(\boldsymbol{x}\cdot\boldsymbol{\mu}_n - a\right)\hat{\boldsymbol{k}} - \left(\boldsymbol{x}\cdot\boldsymbol{\mu}_n + a\right)\boldsymbol{\mu}_n \quad (26)$$

with

$$a = \frac{1}{1+\sqrt{n}}\boldsymbol{x}\cdot\left(\boldsymbol{k}-\boldsymbol{\mu}_n\right) = \frac{1}{1+\sqrt{n}}\sum_{i=1}^{n-1} x_i$$

C. DECOUPLING EQUATIONS AND GEOMETRIC INTERPRETATION

One of the relevant applications of power transformations is the decoupling of variables. This is usually accomplished in a purely algebraic fashion by means of the Clarke matrix (and its variants) or symmetrical components. Unfortunately, this approach causes the underlying geometrical view and interpretation to be completely lost. To highlight this fact, the case of a polyphase induction electrical machine is analysed. The equations in matrix form are as follows: [31]:

$$\begin{aligned}[v_s] &= [R_s][i_s] + \frac{d[\psi_s]}{dt}\\ [v_r] &= [R_r][i_r] + \frac{d[\psi_r]}{dt}\end{aligned} \quad (27)$$

where $[v_s]$ and $[v_r]$ refer to the stator and rotor voltage vectors, respectively. The $[R_s]$ and $[R_r]$ are diagonal matrices of resistances while the flux linkage vector in stator $[\psi_s]$ and rotor $[\psi_r]$ are defined as,

$$\begin{aligned}[\psi_s] &= [L_s][i_s] + [L_{sr}][i_r]\\ [\psi_r] &= [L_r][i_r] + [L_{rs}][i_s]\end{aligned} \quad (28)$$

For symmetric machines and under the UTEM assumptions [32], the inductance matrices $[L_s]$, $[L_r]$, $[L_{sr}]$ and $[L_{rs}]$ are symmetric and circulant [33]. A matrix system can be understood as a linear mapping into an n-dimensional space. Basically, the equations defined in (27) and (28) indicate that the current vector is transformed into a voltage vector through the resistance and inductance matrices. The drawback of this mapping is that it produces a system of equations that is hard to solve because of two factors: a) the equations have variables that are coupled together and b) the vectors involved have an extra dimension that could be eliminated. Clarke's method is one of those that can help to solve the two previous disadvantages under certain conditions, although it does not provide any geometrical intuition about the solution. In contrast, SKR does provide a purely geometrical perspective that can help to a better understanding.

For the sake of simplicity, a seven-phase induction machine example is analyzed. The *geometric rotor* for this seven-phase

system is as follows:

$$\boldsymbol{R}_7 = 1\angle -67.79^\circ \left| \sum_{i=1}^{6} \left(\frac{1}{\sqrt{6}}\right)_{i,7} \right| = 1\angle -67.79^\circ \left| \begin{matrix} \frac{1}{\sqrt{6}}\boldsymbol{\mu}_{1,7} \\ \frac{1}{\sqrt{6}}\boldsymbol{\mu}_{2,7} \\ \frac{1}{\sqrt{6}}\boldsymbol{\mu}_{3,7} \\ \frac{1}{\sqrt{6}}\boldsymbol{\mu}_{4,7} \\ \frac{1}{\sqrt{6}}\boldsymbol{\mu}_{5,7} \\ \frac{1}{\sqrt{6}}\boldsymbol{\mu}_{6,7} \end{matrix} \right|$$

with the corresponding matrix (see eq. (22))

$$M_7 = \begin{pmatrix} a_7 & b_7 & b_7 & b_7 & b_7 & b_7 & -c_7 \\ b_7 & a_7 & b_7 & b_7 & b_7 & b_7 & -c_7 \\ b_7 & b_7 & a_7 & b_7 & b_7 & b_7 & -c_7 \\ b_7 & b_7 & b_7 & a_7 & b_7 & b_7 & -c_7 \\ b_7 & b_7 & b_7 & b_7 & a_7 & b_7 & -c_7 \\ b_7 & b_7 & b_7 & b_7 & b_7 & a_7 & -c_7 \\ c_7 & c_7 & c_7 & c_7 & c_7 & c_7 & c_7 \end{pmatrix}$$

$$a_7 = 1 - \frac{1}{7+\sqrt{7}},\ b_7 = -\frac{1}{7+\sqrt{7}},\ c_7 = \frac{1}{\sqrt{7}}$$

As in previous cases, note the regular structure of the matrix. If we follow the traditional eigenvalue computation of the SKR linear map, we get

$$\begin{aligned} \lambda_1 &= \lambda_2 = \lambda_3 = \lambda_4 = \lambda_5 = 1 \\ \lambda_6 &= \frac{1}{\sqrt{7}} + j\frac{\sqrt{6}}{\sqrt{7}} = \cos(67.79) + j\sin(67.79) \\ \lambda_7 &= \frac{1}{\sqrt{7}} - j\frac{\sqrt{6}}{\sqrt{7}} = \cos(67.79) - j\sin(67.79) \end{aligned}$$

with possible eigenvectors

$$\begin{aligned} \boldsymbol{v}_1 &= (-1, 1, 0, 0, 0, 0, 0) \\ \boldsymbol{v}_2 &= (-1, 0, 1, 0, 0, 0, 0) \\ \boldsymbol{v}_3 &= (-1, 0, 0, 1, 0, 0, 0) \\ \boldsymbol{v}_4 &= (-1, 0, 0, 0, 1, 0, 0) \\ \boldsymbol{v}_5 &= (-1, 0, 0, 0, 0, 1, 0) \\ \boldsymbol{v}_6 &= \frac{j}{\sqrt{6}}\left(1, 1, 1, 1, 1, 1, -j\sqrt{6}\right) \\ &= (0, 0, 0, 0, 0, 0, 1) + \frac{j}{\sqrt{6}}(1, 1, 1, 1, 1, 1, 0) \\ \boldsymbol{v}_7 &= -\frac{j}{\sqrt{6}}\left(1, 1, 1, 1, 1, 1, j\sqrt{6}\right) \\ &= (0, 0, 0, 0, 0, 0, 1) - \frac{j}{\sqrt{6}}(1, 1, 1, 1, 1, 1, 0) \end{aligned}$$

We get five real and two conjugated complex eigenvalues and eigenvectors. The interpretation of this result is somehow challenging. Complex numbers are usually associated with rotations, but it is not clear that this formal complexification would be useful while starting with a real mapping between real vectors. A purely geometrical interpretation would be more interesting. This is provided by the concept of eigenblade (see Appendix E). In this way, we are allowed to rewrite eigenvalues λ_6 and λ_7 as a single eigenvalue λ_B. In the same vein, eigenvectors $\boldsymbol{v}_6$ and $\boldsymbol{v}_7$ can be replaced by the simple eigenblade $\boldsymbol{B}$ while capturing the complex structure (i.e., the ability to square to -1) of these eigenvectors,

$$\begin{aligned} \lambda_B &= 1 \\ \boldsymbol{B} &= \boldsymbol{u} \wedge \boldsymbol{v} = -\frac{1}{\sqrt{6}} \sum_{i=1}^{6} \boldsymbol{\mu}_{i,7} \end{aligned} \tag{29}$$

with

$$\begin{aligned} \boldsymbol{u} &= \Re(\boldsymbol{v}_6) = \boldsymbol{\mu}_7 \\ \boldsymbol{v} &= \Im(\boldsymbol{v}_7) = \frac{1}{\sqrt{6}} \sum_{i=1}^{6} \boldsymbol{\mu}_i \end{aligned} \tag{30}$$

Note that $\boldsymbol{B}$ in (29) is exactly the same as the bivector in (18) encoding the plane of rotation of the *geometric rotor* in (16). Moreover, the angle of rotation θ (the angle between the KV and $\boldsymbol{\mu}_7$) is given by the real or imaginary parts of the original eigenvalues $\lambda_{6,7} = \frac{1}{\sqrt{7}} \pm j\frac{\sqrt{6}}{\sqrt{7}} = \cos\theta \pm j\sin\theta$. Thus, the two conjugate eigen-pairs $(\lambda_6, \boldsymbol{v}_6)$ and $(\lambda_7, \boldsymbol{v}_7)$ encode, in an obscure complex algebra manner, the actual geometrical rotational component of the SKR. Therefore, it is evident that the SKR method is interpreted geometrically as a rotation in the plane defined by $\boldsymbol{B}$ to align the $\hat{\boldsymbol{k}}$ vector (KV) with $\boldsymbol{\mu}_7$. The remaining eigenvectors form a subspace of dimension $n-2$ orthogonal to the bivector $\boldsymbol{B}$ as can be easily verified by taking the inner product between any vector $\boldsymbol{v}_1$ to $\boldsymbol{v}_5$ with $\boldsymbol{B}$. Because they are all equal to one, they form an identity map on the subspace spanned by the corresponding eigenvectors $\boldsymbol{v}_1$ to $\boldsymbol{v}_5$. Due to the excess identity map represented by eigenvalues λ_1 to λ_5, the classical matrix multiplication operation performs many unnecessary arithmetical operations to achieve what a simple rotation can compute using equation (23). This difference in computational time increases rapidly as dimensions get higher.

If the same analysis is carried out with the generalised Clarke transformation proposed by Willems [9], the result is to produce more eigenblades than the SKR method, therefore more orthogonal rotation planes, which implies a greater degree of freedom to produce matrices that achieve a better decoupling between the variables. This is the main advantage of Clarke over SKR at the moment. Future work will be able to analyse this situation and find the efficient set of simple rotations that allow decoupling systems by full diagonalisation of matrices, not only in circulant symmetric matrices whose elements on the diagonal are equal, but also in any other type of matrix, for example, asymmetric systems like in untransposed transmission lines or asymmetrical machines.

V. APPLICATIONS OF SKR METHODOLOGY

A detailed validation of the proposed framework is presented in this section by comparing its results with other widely used methods such as the $p-q$ theory [34], FBD method [21]

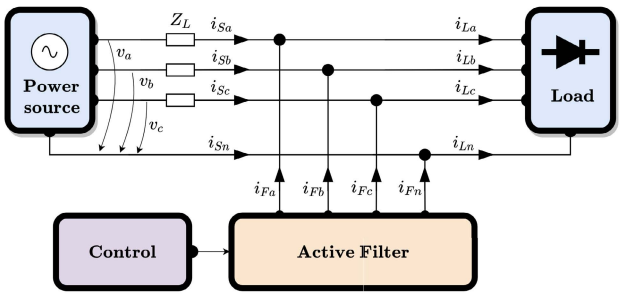

FIGURE 9. Active filter for a three-phase four-wire power system.

TABLE 2. Comparison of RMS current compensation Case #1. values in amperes [A].

	i_a	i_b	i_c	i_n	$\|\|i\|\|$	$\|\|i\|\|^2$
SKR4D	63.15	67.17	63.19	0.72	111.771	12,492.76
FBD	63.15	67.17	63.19	0.72	111.771	12,492.76
SKR3D$_0$	63.26	67.21	63.03	0.00	111.774	12,493.43
Akagi	63.26	67.21	63.03	0.00	111.774	12,493.43
SKR3D	62.81	67.02	63.66	2.88	111.799	12,498.97
Vector	62.81	67.02	63.66	2.88	111.799	12,498.97
Raw	65.21	77.23	60.11	23.26	119.880	14,372.00

and Vector Theory [35], [36]. Current compensation in 4-wire systems with arbitrary voltages is investigated for simplicity, but multi-phase systems with more than 3 phases can be analyzed also. The advantages of our approach rely on obtaining optimal results concerning the energy losses in power transmission considering equal resistances of all the wires. More complex cases can be handled by adding more dimensions.

A. CURRENT COMPENSATION

In order to assess the current compensation operating principles, several real-world examples were analyzed in terms of SKR, Akagi *p-q*, Vector and FBD methodologies. The three-phase four-wire system of Fig. 9 represents a typical scenario where a load is supplied by a power source and an active filter is used to compensate for the current that causes non-active power to flow. The goal is to achieve minimum losses in the transmission line.

1) CASE 1. SCHOOL BUILDING

For the first case under study, a school-type building at the University of Almeria is considered. It consists of several floors with offices, laboratories, and classrooms. The measurements were carried out in the main electrical panel using the openzmeter power quality analyzer and smart energy meter [37]. The three phase-to-neutral voltages as well as the three line and neutral currents were measured. The signals were acquired at 24 kHz and the measurement

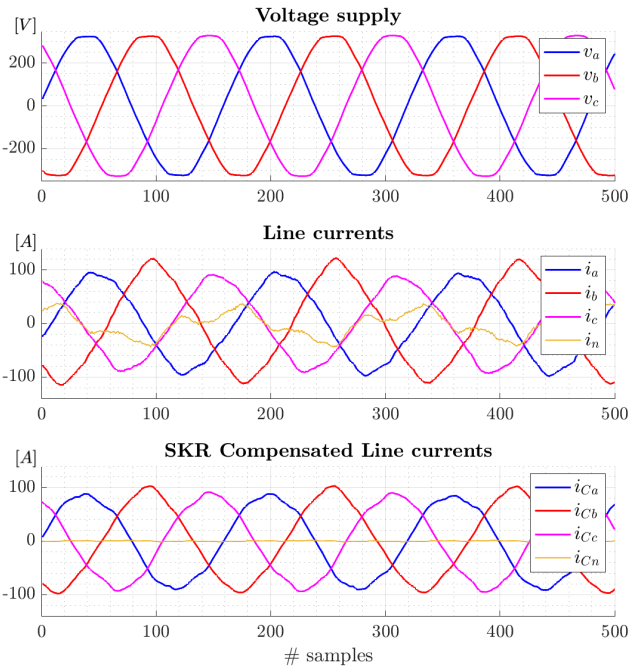

FIGURE 10. Voltage and current waveforms for a school building. Top) voltage supply, middle) source line currents, and bottom) SKR4D line currents.

took several minutes. The active power consumption was 45.55 kW.

The top and middle of Fig. 10 show the voltage and current waveforms for the uncompensated situation, while the bottom shows the compensated current by SKR. Table 2 shows the RMS values of the currents and a loss indicator given by the squared norm of the current vector. It can be seen that the best results are obtained for the 4D SKR method and for FBD. They are optimal by treating all wires equally. Another consequence is that some current is allowed to flow through the neutral wire. In contrast, both Akagi and 3D SKR without zero sequence voltage (SKR3D$_0$) achieve slightly worse results with a null neutral current. Finally, the Vector and the 3D SKR methods give the worst results in terms of losses. In our opinion, this is quite an interesting point. By treating three-phase four-wire systems as 4-dimensional systems, optimal results in terms of transmission losses are achieved.

2) CASE 2. NOISY GRID AND THREE-PHASE INDUCTION MOTOR

The second case of study consists of a typical electrical drive driving a three-phase 4-wire induction motor. The same measurement procedure as in the previous case was performed, acquiring the voltage and current demanded by the electrical drive. In this case, the applied voltage contains a high noise component as well as a high third harmonic. The active power measured during the experiment was 89.79 W. Fig. 11 shows the voltages and currents of the uncompensated load (top and middle, respectively) and the current compensated by the SKR4D method (bottom).

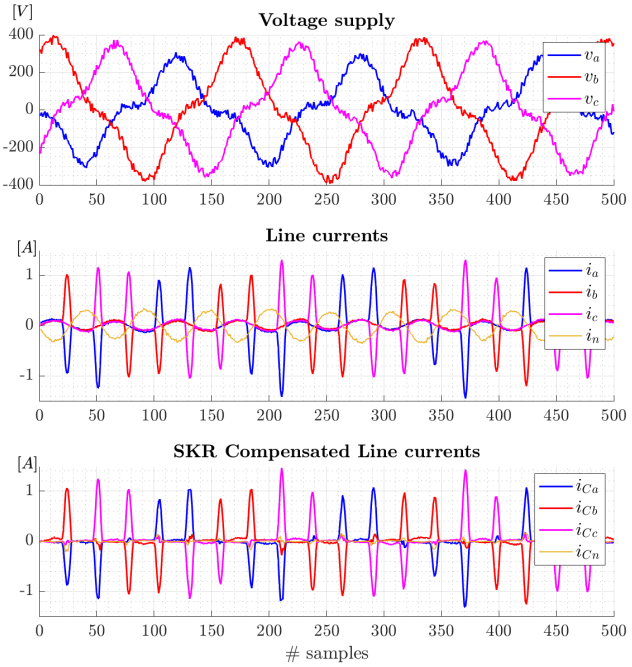

FIGURE 11. Voltage and current waveforms for an electrical drive. Top) voltage supply, middle) line currents, bottom) SKR4D line currents.

TABLE 3. Comparison of RMS current compensation Case #2. Values in milliampere [mA] for the current.

	i_a	i_b	i_c	i_n	$\|i\|$	$\|i\|^2$
SKR4D	306.54	305.96	322.10	35.40	540.91	292,586
FBD	306.54	305.96	322.10	35.40	540.91	292,586
SKR3D$_0$	316.07	301.97	321.25	0.00	542.48	294,285
Akagi	316.07	301.97	321.25	0.00	542.48	294,285
SKR3D	281.91	318.43	327.02	135.09	553.22	306,056
Vector	281.91	318.43	327.02	135.09	553.22	306,056
Raw	346.53	300.84	327.94	247.80	616.07	379,539

Table 3 shows a brief summary of the value of the currents for each stage. It can be seen that, again, the SKR4D and FBD methods outperform all other approaches by using more degrees of freedom and allowing the current to flow through the neutral wire.

B. POWER QUALITY AND GEOMETRY

The use of SKR allows an intuitive understanding of power quality phenomena in three-phase systems in general. In particular, it allows obtaining a three-dimensional visualisation for 4-wire systems which was not possible before. The representation in Fig. 12 shows the spatial trajectory of the transformed SKR voltages $\bar{v}_a$, $\bar{v}_b$ and $\bar{v}_c$ for a three-phase four-wire system in a real building in the University of Almeria. The real voltages were measured from line-to-neutral and afterwards the three line-to-virtual neutral and neutral-to-virtual neutral were computed, i.e., v_{aN}, v_{bN}, v_{cN} and v_{nN}. A total of one hour of measurements were acquired. Colours are used to represent different orbits for every cycle. It can be noticed that the trajectory is almost flat due to the fact that there is not much imbalance between the phases. It can also be seen in the upper left view (perpendicular to the plane formed) that the voltage has a typical hexagonal shape due to the presence of harmonics (specifically harmonics 5 and 7). The upper right view shows the plane viewed from the side where some small deviations can be observed. The lower left view shows another point of view of the setup while the lower right view adds the ideal circular trajectory of a perfectly sinusoidal and balanced voltage. Note how harmonics and unbalance caused by power quality events distort the nominal circle. The application of SKR allows us to reduce the dimensionality of the problem and find a curve with properties related to the electrical quality. For example, for balanced systems, the trajectory describes a circle, while for unbalanced systems, ellipses are formed. This information can be used for detailed analysis of the power quality and to find incipient problems that lead to faults or failures.

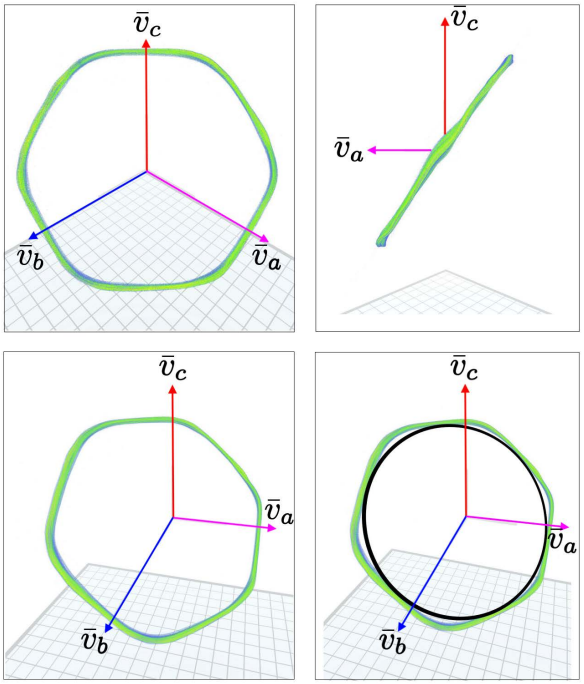

FIGURE 12. SKR applied to a three-phase four-wire line to virtual neutral voltages in a real building. The top left shows an orthogonal view of the plane enclosing the trajectory. The top right image shows a side view of the same trajectory. The bottom left shows a different perspective while the bottom right adds the nominal circle, i.e., the nominal balanced and sinusoidal voltage supply.

VI. CONCLUSION

This paper investigates the generalization of transformations commonly used in electrical engineering by means of Geometric Algebra. For this purpose, the paper formulates some conceptual and computational tools:

- The introduction of new conceptual geometric entities defined in a Euclidean space, such as the Kirchhoff Vector and Kirchhoff Subspace, as well as geometric operators such as *geometric rotors*, leads to the formulation of an orthogonal transformation based on simple rotations (SKR) for any n-dimensional space that circumvents the use of traditional intermediate vector basis, matrices and complex numbers.
- We further reveal how matrix-based electrical transformations can be understood as geometric manipulations of an original orthonormal basis through projections and simple rotations.
- A new efficient implementation of SKR based on linear algebra is also presented, outperforming the classical matrix methods.

The approach taken in this work opens up interesting possibilities to unify different applications in electrical engineering without restriction to a limited number of phases.

- The presented real-world case studies confirm the benefit of the proposed approach. As illustrated by the provided examples, the use of SKR reduces the problem's dimensionality and enables the discovery of a curve with attributes linked to electrical quality, such as the trajectory of balanced and unbalanced systems, and the presence and nature of harmonics. This data can be later utilised to conduct a thorough study of the power quality and identify any problems that could lead to faults or failures.
- Future work should further investigate the application of the proposed SKR model in more complex scenarios in energy engineering disciplines such as compensation, fault analysis, active filtering, multiphase AC machine modelling, and microgrids.
- In addition, new geometric insights should be gathered for the study of other important transformations based on complex numbers such as symmetrical components.

APPENDIX A - CONSTRUCTION OF 3D GEOMETRIC ALGEBRA

In 3-dimensional space $\mathbb{R}^3$, we assume the standard orthonormal basis and denote it as $\boldsymbol{\mu}^{(1)} = \{\boldsymbol{\mu}_1, \boldsymbol{\mu}_2, \boldsymbol{\mu}_3\}$, $\boldsymbol{\mu}_i \cdot \boldsymbol{\mu}_i = 1$, $\boldsymbol{\mu}_i \cdot \boldsymbol{\mu}_j = 0$. One can construct a Euclidean geometric algebra $\mathcal{G}^3$ on $\mathbb{R}^3$ using a new fundamental product of vectors known as *geometric product*. The geometric product is a bilinear, associative, distributive, and non-commutative product on vectors. The geometric product of a basis vector with itself is the same as its inner product $\boldsymbol{\mu}_i\boldsymbol{\mu}_i = \boldsymbol{\mu}_i^2 = \boldsymbol{\mu}_i \cdot \boldsymbol{\mu}_i = 1$. On the other hand, the geometric product of two different basis vectors is a new algebraic element called a basis 2-blade $\boldsymbol{\mu}_i\boldsymbol{\mu}_j$, which satisfies $\boldsymbol{\mu}_i\boldsymbol{\mu}_j = -\boldsymbol{\mu}_j\boldsymbol{\mu}_i$. This new element $\boldsymbol{\mu}_i\boldsymbol{\mu}_j$ (denoted as $\boldsymbol{\mu}_{i,j}$ for short) is an algebraic representation of the 2-dimensional subspace spanned by $\{\boldsymbol{\mu}_i, \boldsymbol{\mu}_j\}$, and accordingly is said to be of grade 2. Using this concept the set of grade 2 basis blades $\boldsymbol{\mu}^{(2)} = \{\boldsymbol{\mu}_{1,2}, \boldsymbol{\mu}_{1,3}, \boldsymbol{\mu}_{2,3}\}$ are constructed. A visual representation of the elements in $\boldsymbol{\mu}^{(1)}$ (the 3 standard unit vectors) and $\boldsymbol{\mu}^{(2)}$ (the 3 perpendicular circles) is shown in Fig. 13. Note that, geometrically, a 2-blade is not a circle. The closest geometric description of a 2-blade is a directed area of arbitrary shape and position, parallel to a given 2-dimensional subspace. This is a geometrically intuitive generalization of the concept of a vector as a directed segment of arbitrary position capable of algebraically representing 1-dimensional subspaces. In this work, circles are used to visualize 2-blades for clarity of illustration. We can use the geometric product once again to define the set of grade 3 basis blades $\boldsymbol{\mu}^{(3)} = \{\boldsymbol{\mu}_{1,2,3}\}$ containing a single algebraic element $\boldsymbol{I} = \boldsymbol{\mu}_{1,2,3}$ which represents the whole 3-dimensional space, visualized as a sphere in Fig. 13. Note that the geometric product of 4 or more basis vectors will not give basis blades of a grade higher than 3. The single element $\boldsymbol{I} = \boldsymbol{\mu}_{1,2,3}$ is called the pseudo-scalar of $\mathcal{G}^3$. Additionally, $\boldsymbol{\mu}^{(0)} = \{1\}$ is used to represent a basis for real numbers as in $\mathbb{R}$. Finally, a basis of 8 blades of mixed grades is obtained for the whole geometric algebra $\mathcal{G}^3$ using $\boldsymbol{\mu} = \boldsymbol{\mu}^{(0)} \cup \boldsymbol{\mu}^{(1)} \cup \boldsymbol{\mu}^{(2)} \cup \boldsymbol{\mu}^{(3)} = \{1, \boldsymbol{\mu}_1, \boldsymbol{\mu}_2, \boldsymbol{\mu}_3, \boldsymbol{\mu}_{1,2}, \boldsymbol{\mu}_{1,3}, \boldsymbol{\mu}_{2,3}, \boldsymbol{\mu}_{1,2,3}\}$. An element $\boldsymbol{A} \in \mathcal{G}^3$ is called a multivector, and is a linear combination of basis blades in $\boldsymbol{\mu}$ with the general form:

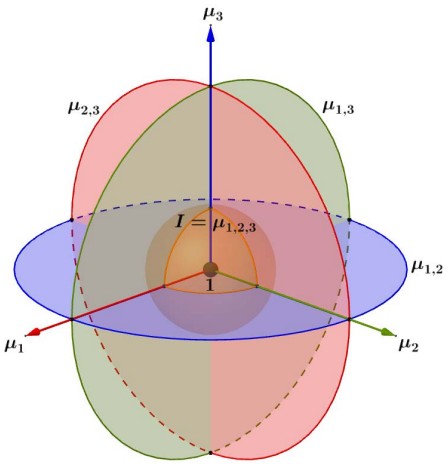

FIGURE 13. Representation of the 8 basis blades for 3-dimensional Euclidean geometric algebra: basis 0-blade/scalar $\{1\}$ (black point at origin), basis 1-blades $\{\mu_1, \mu_2, \mu_3\}$ (red, green, and blue vectors), basis 2-blades $\{\mu_{1,2}, \mu_{1,3}, \mu_{2,3}\}$ (blue, green, and red circles), and basis 3-blade/pseudo-scalar $\{I\} = \{\mu_{1,2,3}\}$ (orange sphere).

$$\begin{aligned}\boldsymbol{A} = a &+ a_1\boldsymbol{\mu}_1 + a_2\boldsymbol{\mu}_2 + a_3\boldsymbol{\mu}_3 \\ &+ a_{1,2}\boldsymbol{\mu}_{1,2} + a_{1,3}\boldsymbol{\mu}_{1,3} + a_{2,3}\boldsymbol{\mu}_{2,3} \\ &+ a_{1,2,3}\boldsymbol{\mu}_{1,2,3}\end{aligned} \tag{A.1}$$

In the above expression, $a_{\dots} \in \mathbb{R}$ are real numbers. Note that the geometric product of two multivectors is another multivector in the same GA; i.e. the set of multivectors is closed under the geometric product, in addition to being closed under linear combinations of multivectors. We can group terms of the same grade in a multivector and express it as $\boldsymbol{A} = \langle \boldsymbol{A} \rangle_0 + \langle \boldsymbol{A} \rangle_1 + \langle \boldsymbol{A} \rangle_2 + \langle \boldsymbol{A} \rangle_3$ where $\langle \boldsymbol{A} \rangle_0 = a$ is its scalar

(or grade 0) part, $\langle \boldsymbol{A} \rangle_1 = a_1\boldsymbol{\mu}_1 + a_2\boldsymbol{\mu}_2 + a_3\boldsymbol{\mu}_3$ is its vector (or grade 1) part, $\langle \boldsymbol{A} \rangle_2 = a_{1,2}\boldsymbol{\mu}_{1,2} + a_{1,3}\boldsymbol{\mu}_{1,3} + a_{2,3}\boldsymbol{\mu}_{2,3}$ is its 2-vector (or grade 2) part, and $\langle \boldsymbol{A} \rangle_3 = a_{1,2,3}\boldsymbol{\mu}_{1,2,3}$ is its 3-vector (or grade 3) part.

APPENDIX B - CONSTRUCTION OF *N*-D GEOMETRIC ALGEBRA

Given a n-dimensional real vector space $\mathbb{R}^n$ defined by an orthonormal vector basis $\boldsymbol{\mu}^{(1)} = \{\boldsymbol{\mu}_1, \boldsymbol{\mu}_2, \ldots, \boldsymbol{\mu}_n\}$, we can construct a set of basis blades $\boldsymbol{\mu} = \bigcup_{i=0}^{n} \boldsymbol{\mu}^{(i)}$ for a Euclidean geometric algebra $\mathcal{G}^n$ using the geometric product. In this general case, we need to define $\boldsymbol{\mu}^{(i)}$ for $i = 2, 3, \ldots, n$, in addition to $\boldsymbol{\mu}^{(0)} = \{1\}$ and the given $\boldsymbol{\mu}^{(1)}$. Each basis blades set $\boldsymbol{\mu}^{(i)}$ of grade i contains exactly $\binom{n}{i} = \frac{n!}{i!(n-i)!}$ elements called basis i-blades.

Each basis i-blade $\boldsymbol{\mu}_{j_1,j_2,\ldots,j_i} \equiv \boldsymbol{\mu}_{j_1}\boldsymbol{\mu}_{j_2}\cdots\boldsymbol{\mu}_{j_i}$ is defined through the application of the geometric product to a unique combination of i basis vectors taken from $\boldsymbol{\mu}^{(1)}$.

As a result, the total number of basis blades in $\boldsymbol{\mu}$ is $\sum_{i=0}^{n}\binom{n}{i} = 2^n$. The n grade basis blade $\boldsymbol{I} = \boldsymbol{\mu}_{1,2,\ldots,n}$ is called the pseudo-scalar of $\mathcal{G}^n$. A multivector $\boldsymbol{A} \in \mathcal{G}^n$ is a linear combination of basis blades in $\boldsymbol{\mu}$. We can group terms of the same grade in a multivector and express it as $\boldsymbol{A} = \sum_{i=0}^{n}\langle \boldsymbol{A} \rangle_i$ where $\langle \boldsymbol{A} \rangle_i$ is called its grade i part. Note that $\langle \boldsymbol{A} \rangle_i = 0$ by definition for $i < 0$ or $i > n$.

Two useful operations on a multivector $\boldsymbol{A} = \sum_{i=0}^{n}\langle \boldsymbol{A} \rangle_i$ are its grade involution $\overline{\boldsymbol{A}}$ and reverse $\boldsymbol{A}^\dagger$ defined as:

$$\overline{\boldsymbol{A}} = \sum_{i=0}^{n}(-1)^i \langle \boldsymbol{A} \rangle_i \tag{B.1}$$

$$\boldsymbol{A}^\dagger = \sum_{i=0}^{n}(-1)^{i(i-1)/2} \langle \boldsymbol{A} \rangle_i \tag{B.2}$$

Note that for a vector $\boldsymbol{a} \in \mathbb{R}^n$ we get $\overline{\boldsymbol{a}} = -\boldsymbol{a}$ and $\boldsymbol{a}^\dagger = \boldsymbol{a}$. This algebraic construction encodes a very rich mathematical structure capable of representing sophisticated geometric models in n-dimensions in a clear way. We can use a special subset of multivectors, called *blades*, to algebraically represent arbitrary subspaces of all dimensions in $\mathbb{R}^n$. Additionally, we can express arbitrary rotations in $\mathbb{R}^n$ using another subset of multivectors called *geometric rotors* (*rotors* for short). Using the geometric product, we can perform a reflection of a vector in a subspace of any dimension as needed. We can also express the projection of a vector into an arbitrary subspace using simple geometric algebra formulations. Such basic operations are extremely helpful in formulating and understanding the proposed geometric model.

APPENDIX C - TRANSFORMATION OPERATORS IN GA

A. LINEAR PROJECTIONS

We can define a geometrically significant product on multivectors derived from the geometric product. This product is called the left-contraction product, and can be computed using:

$$\boldsymbol{A} \rfloor \boldsymbol{B} = \sum_{i=0}^{n}\sum_{j=0}^{n}\left\langle \langle \boldsymbol{A} \rangle_i \langle \boldsymbol{B} \rangle_j \right\rangle_{j-i} \tag{C.1}$$

The left-contraction of two vectors $\boldsymbol{u}, \boldsymbol{v}$ is exactly their inner product $\boldsymbol{u} \rfloor \boldsymbol{v} = \boldsymbol{u} \cdot \boldsymbol{v}$. Many important geometric operations on vectors and subspaces can be expressed using the left contraction. Some classes of multivectors have inverses under the geometric product $\boldsymbol{A}\boldsymbol{A}^{-1} = \boldsymbol{A}^{-1}\boldsymbol{A} = 1$, which can be generally defined using:

$$\boldsymbol{A}^{-1} = \frac{1}{\left\langle \boldsymbol{A}^\dagger \rfloor \boldsymbol{A} \right\rangle_0}\boldsymbol{A}^\dagger \tag{C.2}$$

Note that $\left\langle \boldsymbol{A}^\dagger \rfloor \boldsymbol{A} \right\rangle_0 \in \mathbb{R}$ for any multivector. When $\boldsymbol{A}$ is a blade, then $\boldsymbol{A}^{-1}$ is a scaled version of $\boldsymbol{A}$, which is a blade with the same grade as $\boldsymbol{A}$, and represents the same subspace $\mathcal{A}$. Most notably, vectors are among the main elements having inverses in geometric algebra defined simply using

$$\boldsymbol{v}^{-1} = \frac{1}{\boldsymbol{v} \cdot \boldsymbol{v}}\boldsymbol{v} \tag{C.3}$$

Having a vector $\boldsymbol{a} \in \mathbb{R}^n$, we can construct a blade $\boldsymbol{A}$ of grade $n-1$ which represents the subspace $\mathcal{A}$ orthogonal to $\boldsymbol{a}$ using the dualization (also called orthogonal complement) operation:

$$\begin{aligned} \boldsymbol{A} &= \boldsymbol{a} \rfloor \boldsymbol{I}^{-1} \\ &= (-1)^{n(n-1)/2}\,\boldsymbol{a} \rfloor \boldsymbol{I} \end{aligned} \tag{C.4}$$

In this work, we denote the relation between a subspace $\mathcal{A}$ and a blade $\boldsymbol{A}$, which algebraically represents it, using $\mathcal{A} \propto \boldsymbol{A}$. Accordingly, we can also write $\mathcal{A} \propto \boldsymbol{a} \rfloor \boldsymbol{I}^{-1}$.

We can either use the vector $\boldsymbol{a}$ or its dual blade $\boldsymbol{A}$ to compute the reflection $\boldsymbol{v}'$ of a vector $\boldsymbol{v}$ on subspace $\mathcal{A}$ using:

$$\boldsymbol{v}' = -\overline{\boldsymbol{A}}\boldsymbol{v}\boldsymbol{A}^{-1} = -\boldsymbol{a}\boldsymbol{v}\boldsymbol{a}^{-1} \tag{C.5}$$

The projection $\mathrm{P}_{\boldsymbol{A}}[\boldsymbol{v}]$ of vector $\boldsymbol{v}$ on the $(n-1)$-dimensional subspace $\mathcal{A}$ is computed using any of the following:

$$\mathrm{P}_{\boldsymbol{A}}[\boldsymbol{v}] = \left(\boldsymbol{v} \rfloor \boldsymbol{A}^{-1}\right) \rfloor \boldsymbol{A} = \frac{1}{2}\left(\boldsymbol{v} - \overline{\boldsymbol{A}}\boldsymbol{v}\boldsymbol{A}^{-1}\right) = \frac{1}{2}\left(\boldsymbol{v} - \boldsymbol{a}\boldsymbol{v}\boldsymbol{a}^{-1}\right)$$

Fig. 14 shows a step-by-step representation of these operations in 3 dimensions. Note that for the 3-dimensional case, the cross product of two vectors $\boldsymbol{a} \times \boldsymbol{v}$ is exactly $\boldsymbol{v} \rfloor \boldsymbol{A} = \boldsymbol{v} \rfloor \left(\boldsymbol{a} \rfloor I^{-1}\right)$.

B. SIMPLE ROTATIONS

The geometric framework we propose in this work requires the generalization of complex numbers to geometrically act as rotation operators in n-dimensions without algebraic restrictions. Multiplication with a complex number of unit length $c = e^{\theta i}$ performs a rotation with angle θ in the complex plane $\mathbb{C}$; geometrically equivalent to a rotation in a 2-dimensional real vector space $\mathbb{R}^2$. Geometric algebra

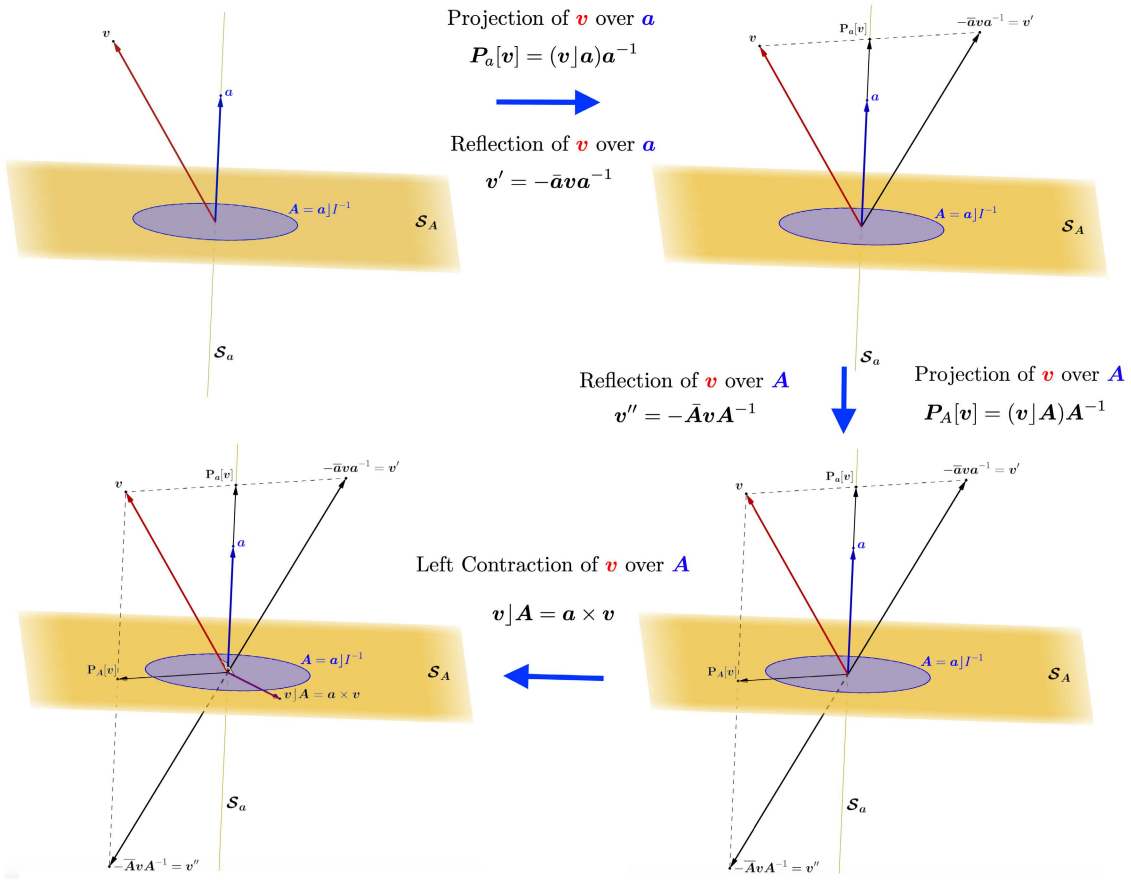

FIGURE 14. Representation of several linear reflection and projection transformations in 3 dimensions. Top left) vector v, a and 2-blade A. Top right) Projection of v over a and reflection of v over a. Bottom right) Projection of v over A and reflection of v over A. Bottom left) Left contraction of v over A (same result as cross product of v and a).

provides a general algebraic alternative for such use of complex numbers using a special class of multivectors called *simplerotors*. In order to properly define a simple *geometricrotor* in n-dimensions, we need to provide an angle of rotation θ and any 2-blade $\boldsymbol{U}$ representing the plane of rotation. The required simple *geometricrotor* is a multivector $\boldsymbol{R} = \langle \boldsymbol{R} \rangle_0 + \langle \boldsymbol{R} \rangle_2$ containing only elements of grades 0 and 2, which can be defined using:

$$\boldsymbol{R} = \cos \tfrac{1}{2}\theta + \sin \tfrac{1}{2}\theta \hat{\boldsymbol{U}} = e^{\frac{1}{2}\theta \hat{U}} \tag{C.6}$$

where $\hat{\boldsymbol{U}} = \frac{1}{\langle \boldsymbol{U} \rfloor \boldsymbol{U} \rangle_0} \boldsymbol{U}$ is a unitary 2-blade. In order to rotate a vector $\boldsymbol{v} \in \mathbb{R}^n$ with angle θ parallel to the 2-dimensional subspace $\mathcal{U}$ represented by $\hat{\boldsymbol{U}}$, the geometric product is applied:

$$\boldsymbol{R}_{\theta,\hat{U}}[\boldsymbol{v}] = \boldsymbol{R}\boldsymbol{v}\boldsymbol{R}^{\dagger} \tag{C.7}$$

In addition, the opposite of a simple rotation transformation is represented by the reverse of its *geometric rotor* $\boldsymbol{R}^{\dagger} = \cos \frac{1}{2}\theta - \sin \frac{1}{2}\theta \hat{\boldsymbol{U}} = e^{-\frac{1}{2}\theta \hat{U}}$:

$$\boldsymbol{R}^{-1}_{\theta,\hat{U}}[\boldsymbol{v}] = \boldsymbol{R}_{-\theta,\hat{U}}[\boldsymbol{v}] = \boldsymbol{R}^{\dagger}\boldsymbol{v}\boldsymbol{R} \tag{C.8}$$

In this work, we will use a special polar notation for simple *geometric rotors* to emphasize their geometric meaning: $\boldsymbol{R} = e^{\frac{1}{2}\theta \hat{U}} \equiv 1\angle\theta \,\big|\, \hat{\boldsymbol{U}}$. This notation is very similar to the polar\phasor notation associated with a complex number of unit length $c = e^{\theta i} \equiv 1\angle\theta$. When $\hat{\boldsymbol{U}}$ is listed as a sum of basis blades of grade 2, we can write them vertically after the vertical separator. For example, for $\hat{\boldsymbol{U}} = 0.267\boldsymbol{\mu}_{1,2} + 0.535\boldsymbol{\mu}_{2,3} + 0.802\boldsymbol{\mu}_{3,1}$ and $\theta = 60°$ one can write the simple *geometric rotor* as:

$$\boldsymbol{R} = 1\angle 60° \left| \begin{matrix} 0.267_{1,2} \\ 0.535_{2,3} \\ 0.802_{3,1} \end{matrix} \right. = 1\angle 60° \,|_{0.267_{1,2}+0.535_{2,3}+0.802_{3,1}}$$

Note that we have omitted the $\boldsymbol{\mu}$ symbol for a more compact notation in this new polar form. Fig. 15 illustrates the main elements of a simple *geometric rotor* in 3 dimensions and the concept of rotation parallel to a plane. Note also that only in 3 dimensions one can define the rotation using an axis $\boldsymbol{u} = \hat{\boldsymbol{U}} \rfloor \boldsymbol{I}^{-1}$. In higher dimensions, however, the orthogonal complement of the rotation 2-blade is not a vector, and the axis representation is not valid.

APPENDIX D - KIRCHHOFF ROTATIONS FAMILY

There is a whole family of rotations that map the basis vector $\boldsymbol{\mu}_n$ to the Kirchhoff vector $\hat{\boldsymbol{k}}$. For example, in three-

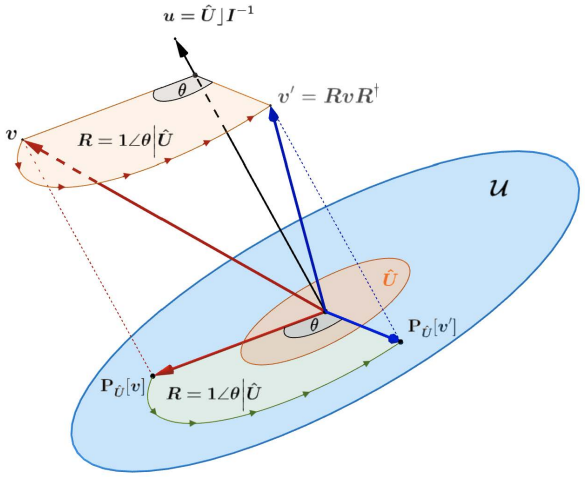

FIGURE 15. Representation of a simple *geometric rotor* $R = 1\angle\theta|\hat{U}$. and its effect on a vector v in 3-dimensional space.

dimensional space, the simplest of them is the SKR rotor defined as:

$$\boldsymbol{R}_3 = 1\angle -54.74^\circ \left| \begin{matrix} \frac{1}{\sqrt{2}}\boldsymbol{\mu}_{1,3} \\ \frac{1}{\sqrt{2}}\boldsymbol{\mu}_{2,3} \end{matrix} \right.$$

Another one of this family is the power-preserving Clarke transformation (in geometric rotor form):

$$\boldsymbol{R}_C = 1\angle -56.6^\circ \left| \begin{matrix} \frac{\sqrt{2}+2}{\sqrt{8\sqrt{3}+2+18}}\boldsymbol{\mu}_{1,3} \\ \frac{1}{\sqrt{4\sqrt{3}+2+9}}\boldsymbol{\mu}_{1,3} \\ \frac{\sqrt{2}+\sqrt{3}}{\sqrt{4\sqrt{3}+2+9}}\boldsymbol{\mu}_{2,3} \end{matrix} \right.$$

The family can be described as a rotor function $\boldsymbol{R}(\theta)$ of a single free parameter $\theta \in \left[-\frac{\pi}{2}, \frac{\pi}{2}\right]$ such that $\hat{\boldsymbol{k}} = \boldsymbol{R}\boldsymbol{\mu}_3\boldsymbol{R}^{\dagger}$. For each rotor $\boldsymbol{R}$ in the family, its angle of rotation is denoted as $\varphi(\theta) \in [\phi, \pi]$ and its unit bivector of rotation is denoted as $\hat{\boldsymbol{N}}(\theta)$, where

$$\phi = \cos^{-1}\left(\boldsymbol{\mu}_3 \cdot \boldsymbol{k}\right) = \cos^{-1}\left(\frac{1}{\sqrt{3}}\right) = 54.74^\circ$$

and $\varphi(\theta) = \varphi(-\theta)$ is an even function in θ with $\varphi(-\frac{\pi}{2}) = \varphi(\frac{\pi}{2}) = \pi$ and $\varphi(0) = \phi$.

The geometry of this method requires the definition of a set of pure rotors

$$\boldsymbol{S}(\theta) = \sqrt{\frac{1}{2}\left(1 + \cos\theta\right)} + \sqrt{\frac{1}{2}\left(1 - \cos\theta\right)}\frac{1}{\sqrt{-\boldsymbol{B}^2}}\boldsymbol{B}$$

where $\boldsymbol{B} = (\hat{\boldsymbol{k}} - \boldsymbol{\mu}_3)^*$ is the 2-blade orthogonal to the difference vector $\hat{\boldsymbol{k}} - \boldsymbol{\mu}_3$. Rotor $\boldsymbol{S}$ performs a rotation in the plane $\boldsymbol{B}$ by an angle $\theta \in \left[-\frac{\pi}{2}, \frac{\pi}{2}\right]$.

The next step in the process requires the use of $\boldsymbol{S}(\theta)$ to perform a rotation of the constant bivector $\boldsymbol{N}$ defined as

$$\boldsymbol{N} = \hat{\boldsymbol{k}} \wedge \boldsymbol{\mu}_3 = \frac{1}{\sqrt{3}}\boldsymbol{\mu}_{1,3} + \frac{1}{\sqrt{3}}\boldsymbol{\mu}_{2,3}$$

to obtain

$$\bar{\boldsymbol{N}}(\theta) = \boldsymbol{S}\left(\hat{\boldsymbol{k}} \wedge \boldsymbol{\mu}_3\right)\boldsymbol{S}^{\dagger} = \left(\boldsymbol{S}\hat{\boldsymbol{k}}\boldsymbol{S}^{\dagger}\right) \wedge \left(\boldsymbol{S}\boldsymbol{\mu}_3\boldsymbol{S}^{\dagger}\right)$$

followed by a projection of $\boldsymbol{\mu}_3$ and $\hat{\boldsymbol{k}}$ on $\bar{\boldsymbol{N}}$ to get

$$\begin{aligned} \boldsymbol{u}(\theta) &= (\boldsymbol{\mu}_3 \rfloor \bar{\boldsymbol{N}}) \rfloor \bar{\boldsymbol{N}}^{-1} \\ \boldsymbol{v}(\theta) &= (\hat{\boldsymbol{k}} \rfloor \bar{\boldsymbol{N}}) \rfloor \bar{\boldsymbol{N}}^{-1} \end{aligned}$$

Finally, the rotor $\boldsymbol{R}(\theta)$ is defined as the rotor that rotates unit vectors $\hat{\boldsymbol{u}}(\theta)$ into $\hat{\boldsymbol{v}}(\theta)$ through the smallest angle between them

$$\varphi(\theta) = \cos^{-1}\left(\hat{\boldsymbol{u}} \cdot \hat{\boldsymbol{v}}\right)$$

After some algebraic manipulations, we can summarize the procedure for defining $\boldsymbol{R}(\theta)$ in the following relations:

$$\begin{aligned} \phi &= \cos^{-1}\left(\frac{1}{\sqrt{3}}\right) \\ \varphi(\theta) &= \cos^{-1}\left(1 + \frac{2\left(1 - \frac{1}{\sqrt{3}}\right)}{\sin^2(\theta)\left(1 + \frac{1}{\sqrt{3}}\right) - 2}\right) \end{aligned}$$

where $-\frac{\pi}{2} \le \theta \le \frac{\pi}{2}$

$$\theta\left(\varphi\right) = \pm\sin^{-1}\sqrt{2\frac{\cos\varphi - \frac{1}{\sqrt{3}}}{\left(1+\frac{1}{\sqrt{3}}\right)(\cos\varphi - 1)}}$$

where $\phi < \varphi < \pi$

$$\begin{aligned} \boldsymbol{S}(\theta) &= \sqrt{\frac{1}{2}\left(1 + \cos\theta\right)} + \sqrt{\frac{1}{2}\left(1 - \cos\theta\right)}\frac{1}{\sqrt{-\boldsymbol{B}^2}}\boldsymbol{B} \\ \boldsymbol{B} &= \left(\boldsymbol{k} - \boldsymbol{\mu}_3\right)^* = \left(\boldsymbol{\mu}_3 - \boldsymbol{k}\right) \rfloor \boldsymbol{\mu}_{1,2,3} \\ \bar{\boldsymbol{N}}(\theta) &= \boldsymbol{S}(\theta)\left(\boldsymbol{k} \wedge \boldsymbol{\mu}_3\right)\boldsymbol{S}^{\dagger}(\theta) \\ &= \frac{1}{\sqrt{3}}\left[\boldsymbol{S}(\theta)\left(\boldsymbol{\mu}_1 + \boldsymbol{\mu}_2\right)\boldsymbol{S}^{\dagger}(\theta)\right] \wedge \left[\boldsymbol{S}(\theta)\boldsymbol{\mu}_3\boldsymbol{S}^{\dagger}(\theta)\right] \\ \hat{\boldsymbol{N}}(\theta) &= \frac{1}{\sqrt{-\bar{\boldsymbol{N}}^2(\theta)}}\bar{\boldsymbol{N}}(\theta) \\ \boldsymbol{R}(\theta) &= \exp\left(\frac{1}{2}\varphi(\theta)\hat{\boldsymbol{N}}(\theta)\right) \\ &= \sqrt{\frac{1}{2}\left(1 + \cos\varphi(\theta)\right)} + \sqrt{\frac{1}{2}\left(1 - \cos\varphi(\theta)\right)}\hat{\boldsymbol{N}}(\theta) \end{aligned}$$

We get the SKR at the smallest rotation angle

$$\varphi = \phi = \cos^{-1}\left(\frac{1}{\sqrt{3}}\right) \Leftrightarrow \theta = \pm\frac{\pi}{2}$$

and the Clarke transformation at a larger angle of

$$\begin{aligned} \varphi &= \cos^{-1}\left(\frac{1}{\sqrt{6}} + \frac{1}{6}\sqrt{3\sqrt{6} + \frac{15}{2}} - \frac{1}{2}\right) = 56.6^\circ \\ \theta &= \pm\sin^{-1}\left(\frac{12\sqrt{2} - 12\sqrt{3} + 6\sqrt{6} - 12}{9\sqrt{2} - 16\sqrt{3} + 5\sqrt{6} - 12}\right) = \pm 0.0758 \end{aligned}$$

We can clearly see the geometric and algebraic simplicity of SKR compared to the Clarke transformation.

APPENDIX E - EIGENVALUES AND EIGENBLADES

In linear algebra, a real square matrix M of size n with determinant ± 1 represents an orthogonal transformation. The eigen-decomposition of such a matrix gives a set of n possibly complex eigen-value\vector pairs $(\lambda_i, \boldsymbol{v}_i) = (\alpha_i + j\beta_i, \boldsymbol{a}_i + j\boldsymbol{b}_i)$. For this case, the following property is always fulfilled

$$|\lambda_i| = \sqrt{\alpha_i^2 + \beta_i^2} = 1$$

Moreover, whenever a complex number $\alpha + j\beta$ is an eigenvalue for $\boldsymbol{M}$, so is its complex conjugate $\alpha - j\beta$.

Geometric algebra provides an intuitive interpretation of these pairs using the concept of eigenblades [38], [39], [40]. For a linear operator $T[\cdot]$, an eigenblade $\boldsymbol{B}$ encodes a subspace $\mathcal{B}$ for which $T[\boldsymbol{x}] = \alpha\boldsymbol{x}$ for all vectors $\boldsymbol{x} \in \mathcal{B}$ using a single real eigenvalue α. For orthogonal transformations, we generally have 3 cases depending on the eigenvalue.

1) The first case is associated with a real eigenvalue $\lambda_i = 1$. In this case, the associated eigenvector $\boldsymbol{v}_i$ encodes a 1-dimensional eigen-subspace where the linear operator performs a simple identity transformation on all vectors in this subspace. By identifying all subspaces with eigenvalues equal to 1, we can safely ignore or skip them during an efficient computation of the linear map.
2) The second case is associated with a real eigenvalue $\lambda_i = -1$. This time, the associated eigenvector encodes a 1-dimensional eigen-subspace where the linear operator performs a reflection on the hyperplane $\boldsymbol{V}_i = \boldsymbol{v}_i \rfloor \boldsymbol{I}_n^{-1}$ orthogonal to $\boldsymbol{v}_i$. This is the most basic set of reflections in linear and geometric algebra as described by Cartan–Dieudonné theorem.
3) Finally, the third case is the complex eigenvalue $\lambda_i = \alpha_i + j\beta_i$, which encodes a rotation inside a 2-dimensional eigen-subspace spanned by the real and imaginary parts of the associated eigenvector $\boldsymbol{v}_i = \boldsymbol{a}_i + j\boldsymbol{b}_i$. The angle of rotation is simply $\theta_i = \tan^{-1}\frac{\beta_i}{\alpha_i}$, and the eigenblade (plane of rotation) is $\boldsymbol{B}_i = \boldsymbol{b}_i \wedge \boldsymbol{a}_i$ [41]. Using this information, a simple geometric rotor could be constructed for each 2-dimensional eigen-subspace of matrix M. Note that the other complex conjugate eigen-pair with value $\lambda_j = \alpha_j - j\beta_j$ must be ignored as it redundantly encodes the same simple rotation, just using different basis vectors.

Combining the above cases together for a given orthogonal transformation matrix, we get a smaller set of orthogonal eigenblades encoding three kinds of basic maps on vectors: identity, simple reflection, and simple rotation. In this way, we can computationally ignore the identity eigen-space, and perform only simple reflections and rotations in any order, due to their orthogonality, using more efficient single loops instead of 3 nested loops of matrix multiplication. Additionally, the geometric interpretation becomes much more obvious compared to interpreting the original complex eigen-pairs of the orthogonal transformation matrix.

REFERENCES

[1] R. S. Herrera, P. Salmerón, and H. Kim, "Instantaneous reactive power theory applied to active power filter compensation: Different approaches, assessment, and experimental results," *IEEE Trans. Ind. Electron.*, vol. 55, no. 1, pp. 184–196, Jan. 2008.
[2] S. Chakraborty and M. G. Simoes, "Experimental evaluation of active filtering in a single-phase high-frequency AC microgrid," *IEEE Trans. Energy Convers.*, vol. 24, no. 3, pp. 673–682, Sep. 2009.
[3] E. Levi, F. Barrero, and M. J. Duran, "Multiphase machines and drives-revisited," *IEEE Trans. Ind. Electron.*, vol. 63, no. 1, pp. 429–432, Oct. 2015.
[4] J. A. B. Faria and J. H. Briceno, "On the modal analysis of asymmetrical three-phase transmission lines using standard transformation matrices," *IEEE Trans. Power Del.*, vol. 12, no. 4, pp. 1760–1765, Oct. 1997.
[5] P. McNamara and F. Milano, "Model predictive control-based AGC for multi-terminal HVDC-connected AC grids," *IEEE Trans. Power Syst.*, vol. 33, no. 1, pp. 1036–1048, Jan. 2017.
[6] F. Milano, "A geometrical interpretation of frequency," *IEEE Trans. Power Syst.*, vol. 37, no. 1, pp. 816–819, Jan. 2022.
[7] O. C. Sakinci and J. Beerten, "Equivalent multiple *dq*-frame model of the MMC using dynamic phasor theory in the $\alpha\beta z$-frame," *IEEE Trans. Power Del.*, vol. 35, no. 6, pp. 2916–2927, Dec. 2020.
[8] C. T. Rim, "Unified general phasor transformation for AC converters," *IEEE Trans. Power Electron.*, vol. 26, no. 9, pp. 2465–2475, Sep. 2011.
[9] J. L. Willems, "Generalized Clarke components for polyphase networks," *IEEE Trans. Educ.*, vol. E-12, no. 1, pp. 69–71, Mar. 1969.
[10] A. Ferrero, L. Giuliani, and J. L. Willems, "A new space-vector transformation for four-conductor systems," *Eur. Trans. Electr. Power*, vol. 10, no. 3, pp. 139–145, Sep. 2007.
[11] G. T. Heydt, "Thévenin's theorem applied to the analysis of polyphase transmission circuits," *IEEE Trans. Power Del.*, vol. 32, no. 1, pp. 72–77, Feb. 2017.
[12] C. J. O'Rourke, M. M. Qasim, M. R. Overlin, and J. L. Kirtley, "A geometric interpretation of reference frames and transformations: dq0, Clarke, and Park," *IEEE Trans. Energy Convers.*, vol. 34, no. 4, pp. 2070–2083, Dec. 2019.
[13] F. G. Montoya and A. H. Eid, "Formulating the geometric foundation of Clarke, Park, and FBD transformations by means of Clifford's geometric algebra," *Math. Methods Appl. Sci.*, vol. 45, no. 8, pp. 4252–4277, May 2021.
[14] F. G. Montoya, R. Baños, A. Alcayde, F. M. Arrabal-Campos, and E. Viciana, "Analysis of non-active power in non-sinusoidal circuits using geometric algebra," *Int. J. Electr. Power Energy Syst.*, vol. 116, Mar. 2020, Art. no. 105541.
[15] F. G. Montoya, R. Baños, A. Alcayde, and F. M. Arrabal-Campos, "A new approach to single-phase systems under sinusoidal and non-sinusoidal supply using geometric algebra," *Electr. Power Syst. Res.*, vol. 189, Dec. 2020, Art. no. 106605.
[16] Y. He, R. Wang, X. Wang, J. Zhou, and Y. Yan, "Novel adaptive filtering algorithms based on higher-order statistics and geometric algebra," *IEEE Access*, vol. 8, pp. 73767–73779, 2020.
[17] E. Bayro-Corrochano, "A survey on quaternion algebra and geometric algebra applications in engineering and computer science 1995–2020," *IEEE Access*, vol. 9, pp. 104326–104355, 2021.
[18] R. Wang, K. Wang, W. Cao, and X. Wang, "Geometric algebra in signal and image processing: A survey," *IEEE Access*, vol. 7, pp. 156315–156325, 2019.
[19] E. Clarke, "Problems solved by modified symmetrical components," *Gen. Electr. Rev.*, vol. 41, nos. 11–12, pp. 488–494, 1938.
[20] R. H. Park, "Two-reaction theory of synchronous machines generalized method of analysis—Part I," *Trans. Amer. Inst. Electr. Eng.*, vol. 48, no. 3, pp. 716–727, Jul. 1929.
[21] M. Depenbrock and V. Staudt, "Hyper space vectors: A new four-quantity extension of space-vector theory," *Eur. Trans. Electr. Power*, vol. 8, no. 4, pp. 241–248, Sep. 2007.
[22] K. Kanatani, *Understanding Geometric Algebra: Hamilton, Grassmann, and Clifford for Computer Vision and Graphics*. Boca Raton, FL, USA: CRC Press, 2015.
[23] L. Dorst, D. Fontijne, and S. Mann, *Geometric Algebra for Computer Science: An Object-Oriented Approach to Geometry*. Amsterdam, The Netherlands: Elsevier, 2010.
[24] D. Hestenes and G. Sobczyk, *Clifford Algebra to Geometric Calculus: A Unified Language for Mathematics and Physics*, vol. 5. Cham, Switzerland: Springer, 1984.

[25] M. Depenbrock, V. Staudt, and H. Wrede, "A theoretical investigation of original and modified instantaneous power theory applied to four-wire systems," *IEEE Trans. Ind. Appl.*, vol. 39, no. 4, pp. 1160–1168, Jul. 2003.
[26] L. Dorst, "The inner products of geometric algebra," in *Applications of Geometric Algebra in Computer Science and Engineering*. Cham, Switzerland: Springer, 2002, pp. 35–46.
[27] H. Fischer, "Generalized space vector transformation," *Electr. Eng.*, vol. 82, no. 6, pp. 279–284, 2000.
[28] J. H. Gallier and J. Quaintance, *Differential Geometry and Lie Groups: A Computational Perspective*, vol. 12. Cham, Switzerland: Springer, 2020.
[29] G. Aragón-González, J. L. Aragón, M. A. Rodríguez-Andrade, and L. Verde-Star, "Reflections, rotations, and Pythagorean numbers," *Adv. Appl. Clifford Algebras*, vol. 19, no. 1, pp. 1–14, Feb. 2009.
[30] F. G. Montoya and A. H. Eid, "Formulating the geometric foundation of clarke, park, and FBD transformations by means of Clifford's geometric algebra," *Math. Methods Appl. Sci.*, vol. 45, no. 8, pp. 4252–4277, May 2022.
[31] B. M. Wilamowski and J. D. Irwin, *Power Electronics and Motor Drives*. Boca Raton, FL, USA: CRC Press, 2018.
[32] D. White and H. Woodson, *Electromechanical Energy Conversion* (M.I.T. Core Curriculum Program in Electrical Engineering). Hoboken, NJ, USA: Wiley, 1959. [Online]. Available: https://books.google.es/books?id=TIfHAAAAIAAJ
[33] J. M. Álvarez, "Analysis of time and space harmonics in symmetrical multiphase induction motor drives by means of vector space decomposition," Ph.D. dissertation, Universidade de Vigo, Vigo, Spain, 2015.
[34] H. Akagi, Y. Kanazawa, and A. Nabae, "Instantaneous reactive power compensators comprising switching devices without energy storage components," *IEEE Trans. Ind. Appl.*, vol. IA-20, no. 3, pp. 625–630, May 1984.
[35] J. L. Willems, "A new interpretation of the Akagi-Nabae power components for nonsinusoidal three-phase situations," *IEEE Trans. Instrum. Meas.*, vol. 41, no. 4, pp. 523–527, Aug. 1992.
[36] F. Z. Peng and J.-S. Lai, "Generalized instantaneous reactive power theory for three-phase power systems," *IEEE Trans. Instrum. Meas.*, vol. 45, no. 1, pp. 293–297, Feb. 1996.
[37] E. Viciana, A. Alcayde, F. Montoya, R. Baños, F. Arrabal-Campos, and F. Manzano-Agugliaro, "An open hardware design for Internet of Things power quality and energy saving solutions," *Sensors*, vol. 19, no. 3, p. 627, Feb. 2019.
[38] D. Hestenes, "The design of linear algebra and geometry," *Acta Applicandae Mathematica*, vol. 23, no. 1, pp. 65–93, 1991.
[39] D. Hestenes and R. Ziegler, "Projective geometry with Clifford algebra," *Acta Applicandae Math.*, vol. 23, pp. 25–63, Apr. 1991.
[40] C. Doran, D. Hestenes, F. Sommen, and N. Van Acker, "Lie groups as spin groups," *J. Math. Phys.*, vol. 34, no. 8, pp. 3642–3669, 1993.
[41] G. Sobczyk, "Linear transformations in unitary geometric algebra," *Found. Phys.*, vol. 23, no. 10, pp. 1375–1385, Oct. 1993.

AHMAD H. EID received the Ph.D. degree in computer engineering from Port-Said University, Egypt, in 2010. He is currently a Lecturer with the Electrical Engineering Department, Faculty of Engineering, Port-Said University. His research interests began with image processing and machine learning, and later shifted to focus on the use of geometric algebra for applied geometric modeling in multidisciplinary engineering domains, and developing efficient software systems for such purposes. His teaching activities include modeling and simulation, computer graphics, machine learning, evolutionary optimization, and computer language design.

FRANCISCO G. MONTOYA received the Ph.D. degree in evolutionary optimization techniques applied to power systems at the University of Granada, in 2009. He is currently a member of the Engineering Department, University of Almería, where he has spent 15 years as a Professor, researching and teaching in areas, such as power systems, energy saving, and evolutionary optimization. He has published more than 90 articles in journals, conferences, and workshops, and also has several publications in books and conference proceedings. He is one of the creators of the geometric algebra power theory applied to power systems in the frequency and time domain (https://www.scopus.com/authid/detail.uri?authorId=7005663229).